Final Report

Grant agreement no.:	228999-2
Project acronym:	SMASH
Project title:	Smart Nanostructured Semiconductors for Energy-Saving Light Solutions
Funding Scheme:	Collaborative Project (CP) - Large-scale integrating project (IP)

Date of latest version of Annex I against which the assessment will be made:

Periodic report:	1st Periodic Report
Period covered:	from M01 to M36 (01. September 2009 - 31. August 2012)

Project co-ordinator name:	Martin Strassburg
Project co-ordinator organisation:	Opto Semiconductors GmbH
Phone:	
Fax:	
E-mail:	martin.strassburg@osram-os.com
Project website address:	www.osram.de

Date of preparation:	20.10.2012 22:00
Version:	

1. Publishable Summary

The concept of SMASH is to bring together complementary expertise across Europe to establish disruptive materials technologies and processes based on nanostructured compound semiconductors to realise the key market drivers for the broad penetration of LEDs into the general lighting market: high efficiency and low cost. This will be achieved by:
Novel low-defect, strain-free nanostructured templates that enable epitaxial growth of LED structures on large area substrates with high efficiency
Arrays of nanorod emitters to realise LEDs with remarkably high efficiencies and unique properties. In this novel approach to solid-state lighting (SSL), light emitting nanorod arrays based on InGaN covering the whole visible spectrum from blue to red will be realized which will be incorporated into a single device for phosphor-free white light emission.
In addition, coreshell concepts for nanorod emitters will be explored that reach a drastic increase of active LED area per substrate.
Both approaches will have a large impact on costs because they allow epitaxial growth on large area, low cost substrates such as Silicon.
Within SMASH these new nanostructured materials and suitable processes will enable the realisation of a new generation of highly-efficient and affordable LEDs required for SSL to be viable for the general lighting market. This will keep Europe at the forefront of the energy-saving SSL business and strengthen its position in the manufacturing supply chain and luminaire business.
Besides their benefits for light sources nanostructured semiconductors are also expected to have substantial impact in other fields, including, for example, solar cells, detectors and biosensors.

2. Summary of Project Achievements

The overall goal of SMASH was to establish new materials solutions and process technologies based on nanostructured gallium nitride based semiconductors, for low-cost, power-efficient light sources for the general lighting market.

All consortium beneficiaries have successfully contributed to the SMASH-goals and achieved remarkable results towards said novel nanorods (NR)-based light emitting structures. The work of each work package resulted in significant progress, even some delays could not been avoided. The lively and professional collaboration between the partners has become a backbone ensuring the achievements of the results. All required technologies have been in place and have proven their capabilities. The achieved results enable the SMASH partners a detailed evaluation of the advantages and disadvantages / challenges of the investigated technology. Based on this, a major conclusion has been that the nanrod technology has made a big leap ahead from early research state. However, to become competable or even better than todays state-f-the-art planar LEDs regarding performance and in particular production yields and costs, further studies such as follow-up public funded projects and internal development projects are necessary (and already on the way).

The results achieved in both nanorod (NR) technology sectors - high brightness and high efficacy LEDs based on defect reduced passive NR (PNR) large-area low cost templates and Phosphor-free white LEDs based on InGaN nano-emitters (NE) - are mostly in agreement with the SMASH objectives of the description of work. Backed by simulation of growth, structural, electronic and optical properties of NR arrays and supported by excellent analytics and process development, a profound understanding of (Al,In,Ga)N NR ensembles has been obtained. Simulation provided e.g. design suggestions for the epi layer stack in NRs, for the arrangement of NRs in an ensemble to support light extraction and color mixing strategies for improved efficiencies. Development of novel etch and passivation processes, epi growth schemes and required modifications to the tools and equipment including development of novel process tools have been made. All this enabled the growth and fabrication of novel LED structures and chips based on position-controlled NRs.

The reduction of threading dislocation density (TDD) ensuing from PNRs enabled to achieve white LEDs with efficacies of 130lm/W and higher. Even though the ambitious goal for GaN on sapphire was approached (best TDD < $3x10^7/cm^2$), the focus was put on the defect reduction for GaN on Silicon large area templates. Finally, fully coalesced 4inch templates with TDDs of $1x10^8/cm^2$ have been obtained. This is almost one order of magnitude lower than SOA.

The compatibility of PNRs with the processes of LED fabrication was demonstrated using LEDs structures grown on GaN on Sapphire templates. Using various phosphor converters, high brightness LEDs with efficacies up to 120lm/W were achieved. Despite the highly complex processes and the delicate strain situation with Silicon substrates (tensile after

MOPVE growth), solving the coalescence issues after NR formation and avoiding extensive cracking remained a key step on the way to meet the final objectives. An MOVPE overgrowth process scheme and an advanced chip process paying attention to the fragility of the PNR templates were developed, but promising material, that should be capable to provide white LEDs chips with efficacies above 130lm/W, was only available late in the project. Hence, demonstrators likely meet the goal will only be produced about 2 months after the end of SMASH.

Paying attention to the current tendencies in commercial LED fabrication, the transfer of PNR approach for defect reduction to 4" silicon wafers has started earlier than scheduled. Thus specific characterization capabilities, processes and technologies have been set in place and contributed to the accelerated schedule. A larger amount of resources was necessary in order to develop high brightness, high efficacy LEDs grown on low-cost, large-area silicon substrates. A significant reduction of the threading dislocation density by almost an order of magnitude below the SOA for GaN on Silicon LEDs has been achieved. Since the usage of defect reduced wafers remained very low, the successful application of these results to high efficacy LEDs is delayed. The respective project goals will be achieved after M36.

Due to the small usage of the wafer and cost-intensive processes, immediate commercial exploitation of the PNR approach for high brightness LEDs is not feasible. Nevertheless, partners specialized on tools and process already started commercial exploitation of their results and academic exploitation (e.g., publication, education, ongoing research) of the results is developing through various routes.

The foundation for the phosphor-less white LED has been developed by nanoemitter growth using MOVPE and MBE techniques. The gap to leading edge material quality and efficiency values have been completely closed due to the SMASH activities putting the partners as a benchmark for disc-like and core-shell nanoemitter (level 2 goal), worldwide. This was enabled by collaborative efforts revealing the details of the nucleation and the growth process and determining the growth conditions for LED structures in position controlled NRs. Nevertheless, the ambitious time schedule could not fully be met for the fabrication of the final demonstrators which is expected a few weeks after the end of the project.

NE have been explored with respect to phosphor-free white light emitting devices and to efficiency improved single color LEDs, e.g., blue emitting core-shell NRs. One of the project highlights is the achievement of long wavelength emitting NR arrays enabling the growth of InGaN nanoLEDs emitting in all primary colors. Hence, it became possible to design and to fabricate all-InGaN Phosphor-free white LEDs. Single color NE based on axial NRs were obtained by MBE growth. Such structures exhibit internal quantum efficiencies (IQE) up to 70%, while the IQE in structures with broad emission bands (to produce white light already in one single NR) were found to be below 10%. Novel chip processes have been developed to fit the 3D character of the structures. Even though these activities suffered from the limited amount of suitable MBE-grown material, the feasibility of all developed processes has been demonstrated before the end of the project and various chip lots are currently processed with single color NE and with white emitting NRs. Assuming similar correlation of IQE and external quantum efficiency (EQE) as in test structures, we expect that the level 1 goals of EQE >5% for single color emitter will be met a few weeks after end of the project.

The core-shell NRs achievements can be seen as the outstanding highlight of the project. All related level 2 goals were met, most of them earlier than planned. Non-polar emission from InGaN 3x MQWs wrapped around the core and an increase of active area by 5x compared to 2D wafer have been obtained.

The potential for commercial exploitation of the NE related results is confirmed by the significant number of filed patents and work in this direction will continue. Nevertheless, the technology is still far from ripeness and further research is necessary prior to product development. Further academic exploitation will be as intense as for the PNRs.

Management activities have been carried out as planned. Interactions between WP leaders and individual SMASH partners have occurred according to specific needs. Furthermore, workshops and exchange of young researchers have been used by SMASH partners to intensify collaboration and knowledge exchange.

Exploitation and dissemination activities are proceeding in accordance to plan. The high number of invited talks at international conferences, a download record for a NR review article from SMASH partners in a scientific journal contribution and a relatively high number of patents and patent applications are a few of the highlights. Above this, two SMASH workshop with contributions of external partners and other leading members of the nanorod community were held and also contributed to the education of young researchers from all SMASH partners.

3. Achievements of RTD Workpackages

Workpackage 1:

This workpackage comprised all activities on the characterization of all nanorods and related structures obtained in the integrated project. Resolving the structural, optical and electro-optical properties of LED structures based on passive nanorod templates and on nanoemitter has been a continuous support for all project partners providing fast feedback to the epitaxial growth and to the chip development.

The tasks have been subdivided in subtasks dedicated to structural and chemical characterization, optical characterization, and electrical and electro-optical characterization. While the determination of the threading dislocation density and the identification of contaminations backed the development of the best coalescence conditions for the passive nanorod templates, the determination of the Indium distribution in and the crystalline quality of the nanorod structures grown by MBE and MOVPE were most important for the nanoemitter development. Furthermore, photonic band gap effects have been studied to validate findings from simulation of photonic crystal structures.

Structural characterization of coalesced GaN templates on passive nanorods, etched nanorods and nanopyramids was of primary importance for the achievement of high quality GaN templates for further planar LED fabrication being one of the main SMASH targets. The concept of these templates is based on the coalescence of nanopyramids grown on etched passive nanorod arrays. WP1 therefore performed investigations in close partnership with WP3 in order to study the strain relaxation of etched nanorods, to assess the structural quality of such templates, to study the microstructure of defects generated at coalescence boundary and to study the morphology of nanopyramids. It was shown that, thanks to nanorod morphology, full strain relaxation occurs in etched rods with aspect ratio higher than 1. Indeed, for a diameter of 250 nm, GaN nanorods are almost fully relaxed from a height of 250 nm whatever the initial compressive (on sapphire) or tensile (on silicon) strain. A specific effort was dedicated by CRHEA to the comparison between nanorod templates coalesced on sapphire and silicon base wafer. The studies were carried out on 500nm thick templates coalesced on top of 2µm high etched nanorod arrays. In both cases, it is noticed that the surface roughness of a 0.5µm coalesced layer is compatible with subsequent LED fabrication. Moreover, compared to their respective initial planar GaN templates, final templates show a better structural quality with lower dislocation density in both cases. While the templates on sapphire remain better as deduced from tilt and twist distributions, the relative improvement compared to initial template is larger for nanorod templates on silicon base wafer.

E.g., TEM investigations revealed the defect microstructure of GaN coalesced nanorod templates and allowed to compare the case of coalescence on nanorod arrays with point to point and edge to edge configuration. For 3 microns thick coalesced layer on top of an array of 0.5 micron high rods etched from a planar GaN layer, coalescence induces two kinds of planar defects, i.e. basal plane stacking faults and prismatic plane boundaries which come from the bottom of the coalesced layer. Some basal plane stacking faults terminate at

coalesced boundary. In the case of edge to edge orientation, mixed and edge dislocations are regenerated at coalesced boundary and propagate to the top surface. Higher threading dislocation density is thus observed in the case of this configuration. Additional characteristic microstructures are found in edge to edge configuration such as voids and bending of dislocations coming from the initial nanorod array. Moreover, CRHEA noticed on SEM images of GaN pyramids just after coalescence that asymmetry of the array might result in additional dislocations due to pyramids misalignment. All these observations give indications on the favorable configuration to increase coalesced layer quality. Planar defects observed near the coalescence boundary were identified by PDI as prismatic stacking faults terminated by two basal stacking faults bounded by partial dislocations.Thanks to experimental and simulated HRTEM images, it was possible to discriminate between two possible models of atomic arrangement of prismatic stacking faults in wurtzite (cf. Figure 1).

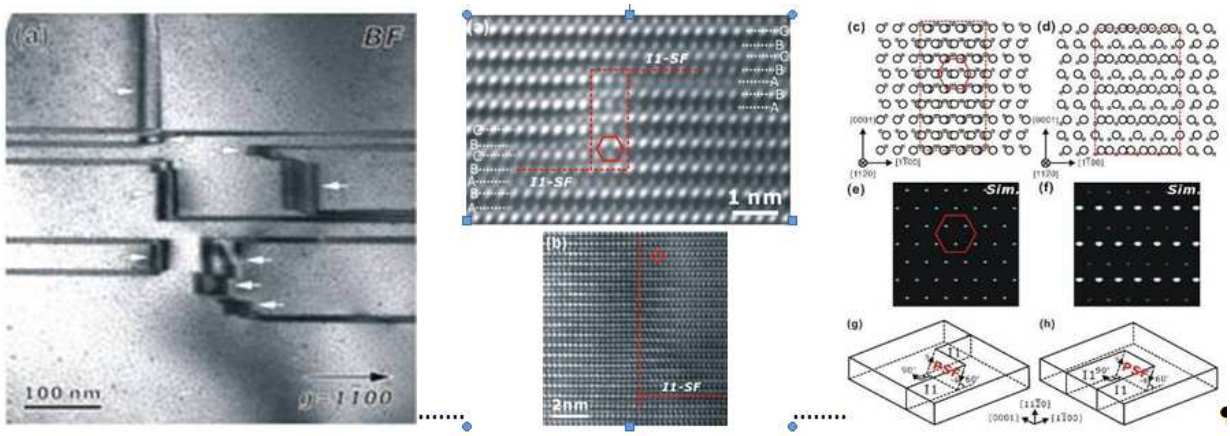

Figure 1 - Planar defects near coalescence boundary. Left : Bright-field TEM image showing arrangements of basal prismatic plane stacking faults near the coalescence boundary taken with g=1-100. The white arrows indicate prismatic stacking faults. High-resolution TEM images of two SF-configurations: step- (a) and hairpin-shaped (b) case. Atomic models proposed by Drum (c) and Amelinckx (d) of the inclined prismatic stacking fault. Simulated HRTEM images in (e) and (f) corresponding to the atomic models of (c) and (d). Three-dimensional schematic drawings of these structures are given in (g) and (h).

Structural and chemical analysis was realized by PDI on MBE-grown InGaN/GaN nanorod grown ordered on Ti masked GaN/Al2O3 templates aiming for broad band emission. They consist of a GaN base followed by 3 sections of InxGa1-x N with increasing In concentration (cf. Figure 2a). The sample presents uniform pencil-like morphology and nanorod diameter as well as the absence of basal plane stacking faults. As shown by STEM image of Figure 2 b), the upper part of the nanorods shows 3 InGaN layers which differ in size and shape. In concentration and spatial distribution was quantified along the axial and radial directions by low-loss electron energy-loss spectroscopy (EELS). Along the axial direction, an increase of the In concentration is determined as expected from the nominal growth conditions (x1<x2<x3) reaching up to 30-40% at the top region of the tip. In Figure 2 c), a step-like variation of the In content is discernable in accordance with the three regions of InxGa1-xN : (I) x1 ≈ 5%, (II) x2 ≈ 15% and (III) x3 ≈ 40%. Furthermore, transverse scan reveals a non-constant behavior with a minimum In content at the rod center.

Most of the nanorods are free of extended defects but a small number of them present a columnar defect with a diameter less than 10nm close to the rod center (cf. Figure 2 d) which is identified as an inversion domain (ID) by TEM analysis. Convergent-Beam Electron Diffraction (CBED) analysis shows that the nanorod region around the defect is Ga-polar while inversion domain is N-polar. The study of the nucleation site of the ID showed that, at the basal plane inversion domain boundary (IDB), an additional layer on the root of (0001) plane is present between the ID and the GaN nanorod matrix. Moreover, local EELS analysis shows a Ti enrichment at basal plane IDB while Ti concentration is below detection limit in the vincinity. PDI proposed an atomic model for GaN homoepitaxial interface. The polarity flip induced by Ti impurity is observed on ordered GaN-polar nanorods both on Ga-polar GaN template on sapphire and on N-polar GaN template on Si(111). The impact of ID on the subsequent In incorporation in InGaN was investigated. The In incorporation is higher for N-polar ID than for Ga-polar nanorod matrix. Mixed polarity InGaN nanorods therefore present a large inhomogeneous In distribution within the nanorods.

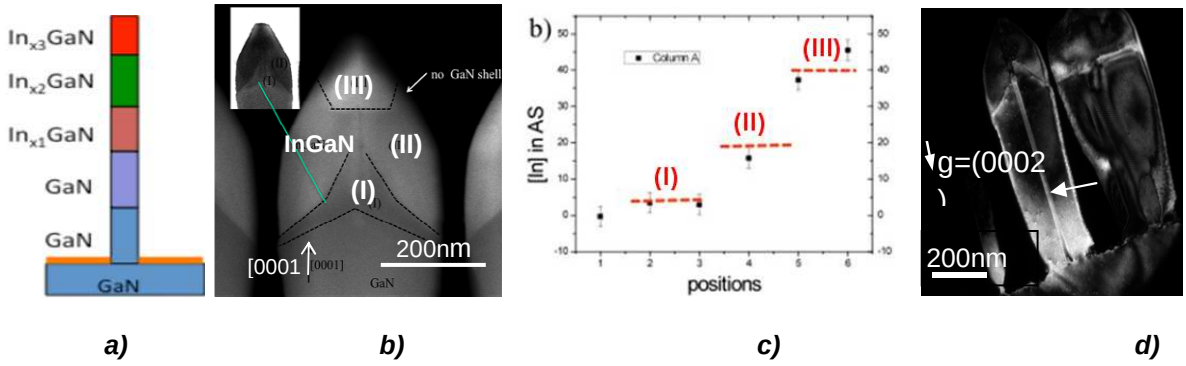

Figure 2 - *STEM images and chemical analysis of an InGaN/GaN nanorod with 3 sections of increasing In content. Nanorod from an ordered array MBE grown on structured GaN template.* ***a)*** *Schematic drawing of the structure* ($x_1<x_2<x_3$) ***b)*** *Magnified HAADF image identifying the three regions (I- II - III) with increasing In content. Inset: Bright-field image of the same area : darker contrast is related to strain.* ***c)*** *Axial EELS line scan showing In content of the 3 regions. Step size between 2 positions is 30-50 nm* ***d)*** *(000-2) dark-field TEM image of a nanorod with an inversion domain (marked with a white arrow)*

WP1 contributed to the effort to demonstrate the achievement of rod arrays with core-shell LED heterostructure and high aspect ratio grown by Metal Organic Vapor Phase Deposition (MOVPE) at TUBS and OSRAM. This section presents investigations on the polarity of the rods grown by selective area growth (SAG) on mask patterned substrates and on their microstructure, especially in the shell region with LED heterostructure.

Rods were grown by SAG-MOVPE on patterned sapphire substrate using SiO2 as mask with a quintuple multi quantum well (MQW) InGaN/GaN core-shell structure.

The nucleation side of position controlled MOVPE-grown nanrods was studied at TUBS after transferring rod arrays in silver powder and removing the growth substrate. As shown in Figure 3 a), in this flipped configuration, two topography domains are observed on the bottom side: the inner part is nucleated at the sapphire surface in patterned holes of the selective SiO2 passivation layer, and the outer part is originated from passivated areas. Analysis of

the nucleation side by Kelvin Probe Force Microscopy (KPFM) (Figure 3 c) and time resolved Surface Photovoltage show that inner and outer parts are Ga-polar and N-polar, respectively. As the sample was flipped, the original GaN rods have then N-polar inner part and Ga-polar outer part regarding the growth direction.

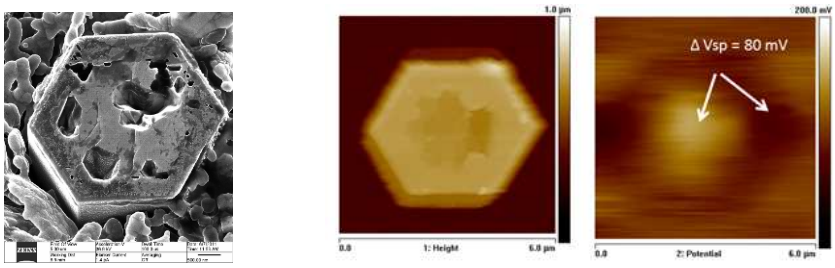

a) ***b)*** ***c)***

Figure 3 – *Nucleation side of mixed polarity core-shell LED rod grown on SiO2 mask patterned sapphire.* ***a)*** *Images with an Helium Ion Microscope on a flipped core-shell LED rod sticking in Ag powder. AFM topography map* ***(b)*** *and corresponding KPFM suface potential map* ***(c)*** *of the nucleation side from flipped GaN core-shell LED rods showing a inner and outer domain. Nominal mask opening D=2µm*

PDI confirmed the mixed polarity of these rods by STEM observations that show inversion domain boundaries. TEM investigations also proved that InGaN quantum wells can be detected along all facets creating a complete core-shell structure. Intensity profile of bright field TEM images across the multi-QW structure reveals that although the 5 QWs have very similar thickness, the barrier thickness varies significantly. Moreover, it indicates In content variation from a QW to another

Nanorods with core-shell geometry including InGaN/GaN MQWs were grown on SiO2 mask patterned GaN/Al2O3 template by position-controlled-MOVPE and their microstructure was investigated by TEM at PDI. Typical NRs with a diameter of 230nm exhibit different facet angles at top and well defined m-plane side facets. Most of nanorods are free of extended defects. Nanorods were grown on GaN templates with different Si doping levels. TEM shows that low Si doping level leads to a smooth interface, while the one realized under high doping level presents a dark zigzag shaped band due to impurities. It is probably due to the high Si concentration. Interestingly, threading dislocations penetrating the template stop at the zigzag line and are bent into the homo-interface.

Optical Characterizations

WP1 continued photoluminescence (PL) and cathodoluminescence (CL) characterization to investigate quality of etched nanorods, nanopyramid properties grown on GaN nanodash templates and coalesced templates in close partnership with WP3.

It was shown that etched nanorods are fully relaxed (Figure 4). However, some strain is recovered during coalescence overgrowth as expected. Strain relaxation in nanorod templates on 4'' Si substrate was studied by CRHEA as function of GaN thickness deposited

on nanorod array. Photoluminescence measurements have been used to determine GaN strain state thanks to emission energy of GaN near band edge. Results show that for a thin layer, just after coalescence, GaN is in tensile strain. Evidence of a partial strain relaxation is observed for a 500nm thick layer. For a thicker layer from 2.5 µm, further strain relaxation occurs and full relaxation is achieved for a 5.5 µm thick layer

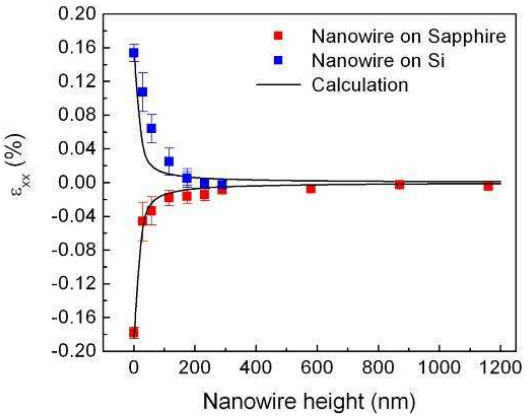

Figure 4 – *Determination of remaining strain on top of the nanorods as a function of their height for a given diameter of 200nm. Independent of the applied initial strain in the layer (compressive or tensile), a full relaxation of the inbuilt strain was obtained with nanorods of an aspect ratio of one ore above.*

PDI investigated the cathodoluminescence (CL) of MBE-grown InGaN/GaN nanorods. The CL of a sample that consists of nanorods with a GaN base followed by 3 sections of InxGa1-x N with increasing In concentration. The spectrum presents a broad luminescence in the wavelength range between 500 and 600 nm which is attributed to the incorporation of In as demonstrated by the corresponding CL maps. Emission with longer wavelength corresponds to regions closer to the top of the rods, which is in agreement with the EELS results of an increase in the In content. However, the spatial resolution of the CL measurement is not sufficient to distinguish between the three regions. Micro-photoluminescence (µPL) at room temperature has also been investigated on samples from TUBS and UPM. The set-up is based on a confocal microscope using a 350nm laser excitation with a spatial resolution of ~ 500nm.

In the frame of WP4, nanorod ordered arrays with InGaN section on top of GaN base have been grown by MBE on GaN templates on sapphire in different conditions to monitor In content and therefore emission spectral distribution. Indeed, non resonant photoluminescence has been used to characterize InGaN band of blue, green and “red” narrow emitters as well as broad band emitters obtained either by gradual variation of In content or sequential deposition of blue, green and “red” sections. Variation of spectra from low temperature to room temperature allowed to evaluate Internal Quantum Efficiency (IQE) of InGaN/GaN nanostructures with narrow band emission. The PL of samples with ordered p-i-n nanoemitters with fixed composition (single colors, centered in the blue and green respectively) and one with broader emission (whitish) with an InGaN section with a gradient In composition was evaluated by UPM. The IQE values obtained from these samples are quite high for the first two with fixed In composition (around 40%) but not so for the one with the broad emission (around 2%)

WP1 investigations on nanoLED devices were based on EBIC and EL measurements. The few available samples were characterized by TUBS using probe tips on single nanoemitters. For several samples grown by MOVPE inside WP4, the core-shell geometry of the depletion region was proven by electron beam induced current (EBIC) measurements at TUBS. This is evidenced in Figure 5 a) in the “lucky” case of a cleaved core-shell LED structure on sapphire that could be directly contacted to n-GaN and p-GaN shell by two probe tips.

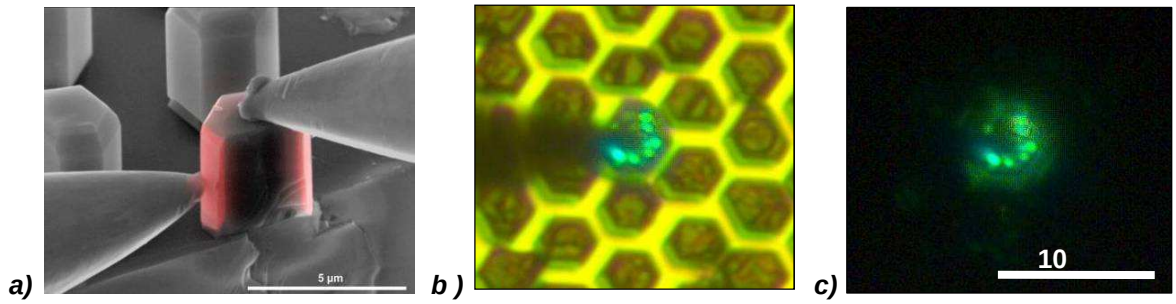

Figure 5 – EBIC and EL characterization of core-shell LED structure on sapphire. **a)** SE image with EBIC overlay (red) of a cleaved core-shell LED structure on sapphire contacted by two probe tips at a reverse bias voltage of V_R= 5 V performed at TUBS. Unlike to the neighbor structures the p-GaN on top and the front part of the structure is removed by cleaving the substrate. **b)** and **c)** Optical microscope image of a core-shell LED and EL emission pattern at a current of I_{tip}= +30 µA. The top facet is contacted by a probe tip and the second contact is performed by an evaporated and processed Ag layer present on the substrate and bottom part of the sidewalls.

Such EBIC measurements are also performed in a p-n-p configuration on complete core-shell structures without further processing. While using a bias voltage, the EBIC is collected by the contact of the backward driven pn-junction. These electrical characterization performed by TUBS in addition prove the conjunct p-type shell around an n-type core. The reduced EBIC signal on r-planes is probably due to a thin and hence depleted p-GaN.

On this sample also locally resolved EL was observed in such a contact scheme. According to the current direction this EL can be assigned to the forward driven pn-junction on the top facet or the sidewall. EL in this contact configuration is more stable than a direct contact by two probe tips (Figure 5 b) and c).

As the optimization of a photonic crystal (PhC) structure is generally complicated and validation of numerical model / simulation results is an important factor in improving accuracy of the model, the experimental research effort has been concentrated to further development of tools for reliable identification of 2D PhC photonic bands. It is well known the principal possibility to measure experimentally photonic single band gaps even without light coupling inside the periodic surface structure by applying of angle-resolved spectroscopy. A novel approach how to evaluate the resonant features on 2D photonic structures has been proposed.

The procedure is based on the idea of recording the set of spectra at the defined angles of illumination by rotating the periodic structure sample around the axis perpendicular to the surface. Experiments were performed by an optical scheme where the light specularly

reflected from the surface periodic structure was detected and spectrally decomposed. As it was shown the predictability of the resonant peaks traces is better and also the contrast of mapping is much more enhanced comparing the angle-resolved spectroscopy (Figure 6).

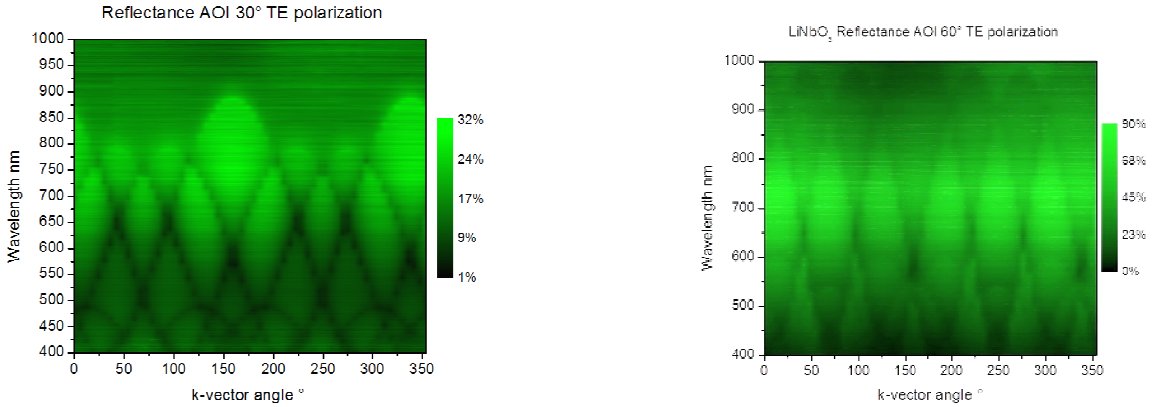

Figure 6 - Spectrally-resolved reflectance obtained by rotating the sample of 2D photonic crystal around the axis perpendicular to the plane of periodic structure at two different angles of illumination. The photonic crystal is hexagonal structure of $LiNbO_3$ nanorods. The period of the structure is 600 nm and the height of nanorods is 220 nm.

Workpackage 2:

Task 2.1: Relation between the physical structure of the rods and the electronic band structure

At UTV, the multiscale simulation tool TiberCAD (www.tibercad.org) has been upgraded and extended according to the requirement of the SMASH project. The simulation tool includes all the relevant physical models, both at continuous and atomistic level, for the investigation of strain, transport and opto/electronic properties of GaN nanocolumn structures. An accurate tuning of the relevant material parameters has been performed for a correct calibration of the simulation tools. Strain maps and the effects of strain, piezo and spontaneous polarizations, as well as surface states, on band profiles have been studied in GaN nanocolumn p-i-n diode structures with different active regions, such as Quantum Disk (QD), Core Shell, and Pencil nanocolumns. The interplay between size, shape and In content of the active region has been pointed out. Electron and hole states of the QD have been calculated, both with an EFA k·p model and an empirical tight-binding (TB) atomistic model. Self consistent band profiles have been calculated by concurrently solving the Poisson/drift-diffusion and the quantum mechanical models. Optical emission spectra and the dependence of transition energies on geometrical and material parameters have been analyzed.

Task 2.2: Carrier transport through the nanorods

Here, two approaches have been pursued. At UTV the TiberCAD tool has been extended for analyzing carrier transport, and at UKAS the tool Quatra/cels has been developed which models carrier transport with a modified drift-diffusion/quantum mechanical approach. These models enable the study of internal quantum efficiency, current-voltage relationship and electroluminescence dependent on pn-junction placement (core/shell vs. quantum-disk), rod dimensions (height/diameter), and contacting scheme (top/side contact). Special focus has been put on surface effects, as the surface to volume ratio is large for nanometer sized devices. As conclusion, the fundamental physical mechanisms governing the device characteristics have been clarified. Details of these findings are summarized in task 2.4

Task 2.3: Optical Properties of Nanorods

Here, an FDTD-based full-wave optical computation of the optical properties has been developed. The method solves the vectorial Maxwell equations in time domain for a three-dimensional representation of the Nano-LED. Figure 2.1 shows a sketch of such a simulation domain for a nanorod device, containing a metallic backside mirror, an array of NRs embedded in filling material, a coalesced layer of GaN and a layer of the adjacent ambient material. The NRs may either have quantum-disc or core-shell geometry. Additionally, the top surface may feature a thin-film typical surface roughness to improve light extraction.

Emission and absorption parameters of the active layers are taken from the electronic band structure computations (see task 2.1) and are used as an input to the optical simulations. As an output we get device related relevant properties, which are the Purcell factor F_P, the optical extraction rate β, the absorption rate in the mirror χ_{mirror} and the re-absorption rate γ. This allows computation of the extraction efficiency, with all the relevant coupling mechanisms included.

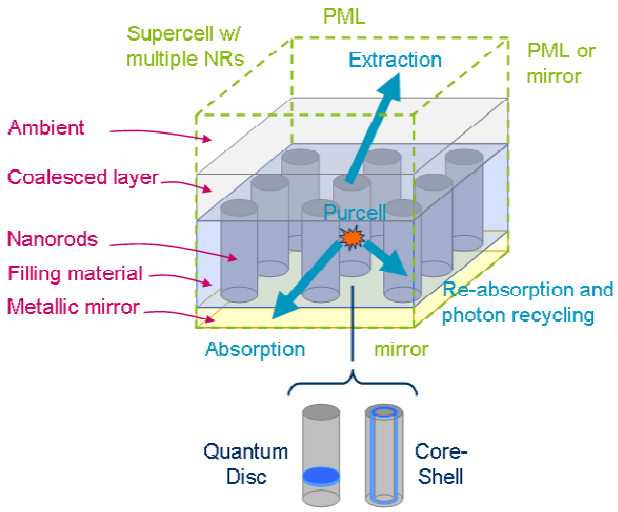

Figure 1: Sketch of the optoelectronic model. Geometry objects are labeled in red, boundary conditions in green, output quantities in blue.

Task 2.4: Device properties of nanorod LEDs

Monochromatic Core-Shell NR LEDs

a.) General Design Aspects

In monochromatic core-shell (CS) nanorod (NR) LEDs, the main feature is aimed at external efficiency improvement at high chip current density in order to overcome the droop effect. This is realized by enlarging the effective active area of the LED with the vertical junction at the sidewalls of the NR. The active area per chip area can be improved which is illustrated in Fig. 2, left. Realistic area factors can be up to 20.

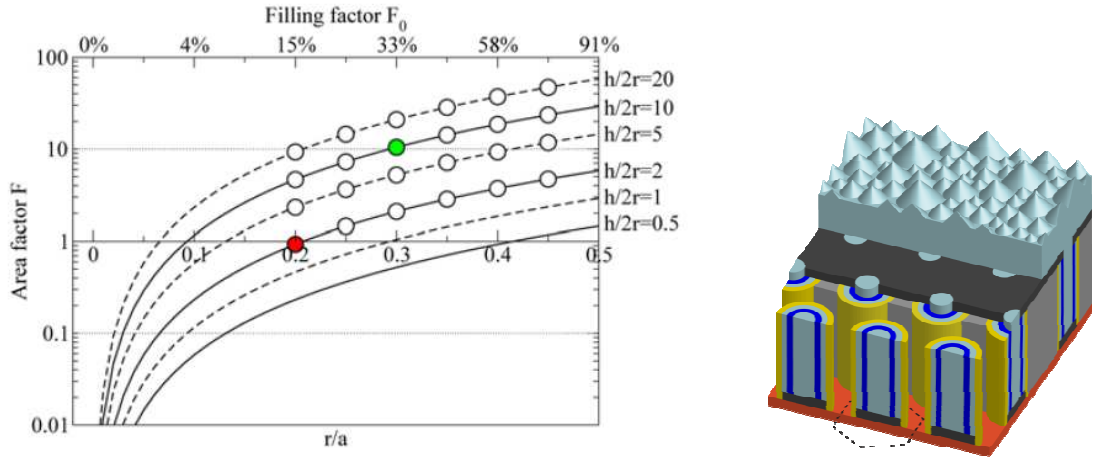

Fig. 2: Left: Active area enhancement factor F as a function of the NR density (r/a or filling factor F0) and the aspect ratio (h/2r) at an active shell radius of ρ/r=0.8. Red and green points represent geometries with an area factor of F=1 and F=10, respectively. Right: Sketch of the geometry of a core-shell nanorod LED.

For an assessment of the current scaling capability, the internal quantum efficiency as well as the extraction efficiency have been analyzed. The former is achieved by the electronic

model (from task 2.2), the latter by the optical model (task 2.3). As goal, the general performance limits for electroluminescence, and the optimum designs are obtained by means of detailed simulation.

b.) Electronic model and electroluminescence spectrum

The coupled classical/quantum models Quatra/cels and TiberCad have been applied to core-shell structures in order to calculate the internal quantum efficiency (IQE). In a first investigation, the contacting scheme has been investigated. As main result, optimum IQE can only be obtained with transparent p-contacts at the sidewalls of the p-shell (see progress report M19-36, WP2). It has been assumed that the core is n-type and the shell is p-type (see Fig. 2, right). Fig. 3 shows the IQE for a nanorod LED with different aspect ratios, with a core radius of 350 nm, and a shell thickness of 200 nm. The current density is calculated relative to the nanorod surface area.

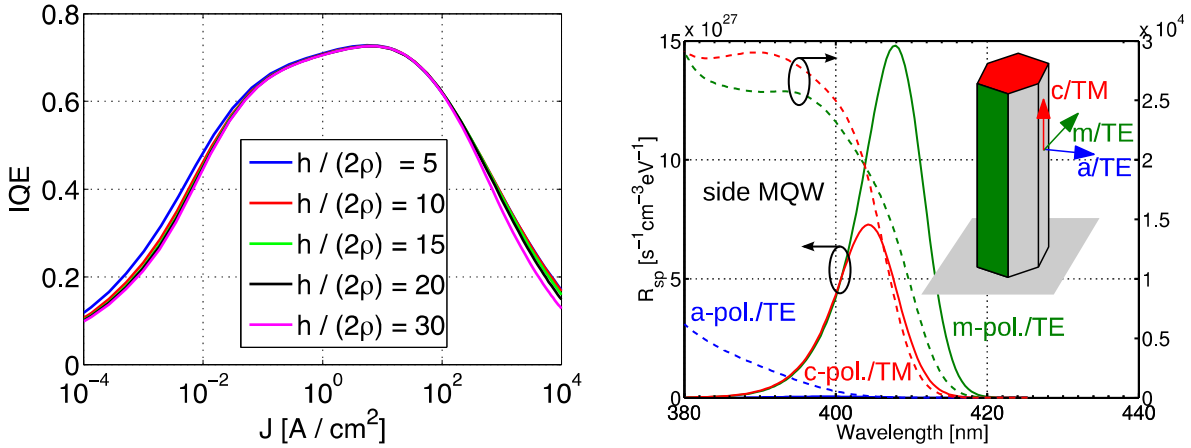

Fig. 3: left: IQE calculated for a NR LED with varying height versus current per nanorod surface area. The drooping at high current density does not change; which allows scaling of the efficiency maximum in a nanorod array. Right: Anisotropic luminescence spectra and absorption of a CSN LED with h/d = 5 and cap contact at I = 3.5·10⁻⁶A. Shown are the averaged radiative recombination rate of the electroluminescence spectrum (continuous line) and absorption (dashed line) for each principal axis.

Based on these results, the IQE curve can be scaled on the current axis by scaling the active area vs. the chip area without significant loss of efficiency. Modification of the rod dimensions shows that down to a core radius of 50nm and shell thickness of 50nm this statement is valid.

On the right figure in Fig. 3, the optical emission and absorption spectra are plotted. Those spectra differ significantly from thin-film structures, as they are highly anisotropic, and the absorption is much larger than in the thin-film case due to the a-plane orientation of the shell sidewall quantum wells. Those data serve as input to the optical simulation described in section c.

Parametric Study and optimization of the Core Shell geometry

A circular core-shell MQW structure (see Fig. 4) has been simulated classically using the Drift-Diffusion model and the classical IQE has been extracted for different contact configurations, with and without electron blocking layer (EBL) and with surface recombination

(Partner UTV). The QWs are 3 nm wide In0.1Ga0.9N wells with 8 nm GaN barriers. For the device including an AlGaN EBL, both EBL and p-contact regions are p-type doped with doping density of 5x1018 cm-3.

Fig. 5 shows the resulting IQE for the four different simulations. The first two cases refer to a structure without electron blocking layer, but having different anode configuration. As can be seen from the figure, the lateral anode leads to a severely reduced IQE compared to the top anode. This is due to the fact that electrons escape the MQW region and recombine on the nearby anode. If the device is contacted at the top, the carriers are forced to move vertically what they preferably do inside the quantum wells. This leads to less electron leakage and to higher radiative recombination in the active layer, and thus to increased IQE.

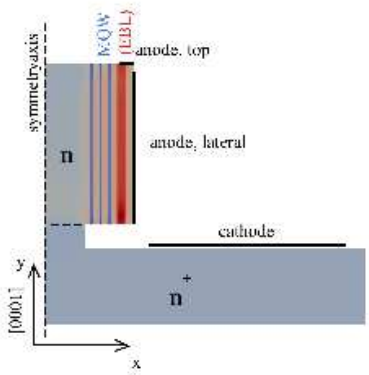

Fig.4 Model of the circular core shell MQW structure, indicating the different simulated contact configurations (lateral and top anode, respectively)

As in standard planar QW structures, electron leakage can be suppressed by growing an AlGaN EBL before the p contact layer. The simulated IQE including a 10 nm Al0.15Ga0.85N EBL shows considerable improvement in IQE due to suppressed electron leakage. The latter can be seen in Fig. 3, showing the x-component of the electron current density along the radius (x-axis) in the lower part of the column.

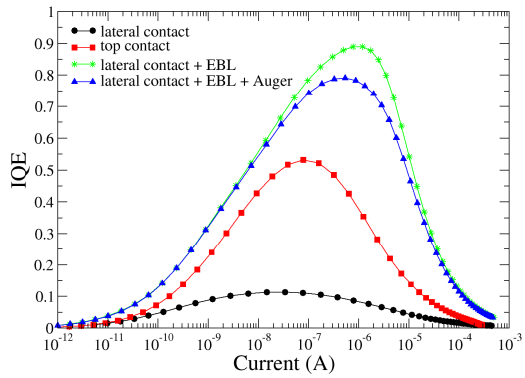

Fig. 5 Classical IQE for the different configurations

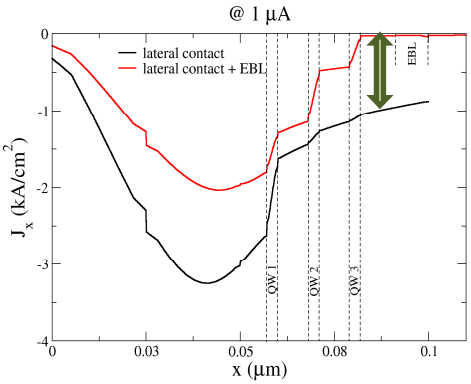

Fig.6 x-component of the electron current density along the radius. The green arrow highlights the amount of electron leakage without EBL.

A full parametric study with different Indium contents, contact placements, and surface terminations has been carried out, in order to find the maximum efficiency design. In addition, partner UTV has carried out atomistic empirical tight binding band structure calculations for an axial nano rod structure incorporated in a multi-scale simulation approach.

c.) Optical Model

Applying the optical model, the performance potential of monochromatic, blue emitting core-shell NR LEDs was estimated, including both internal losses and optical effects. Photon recycling and absorption in the required current spreading shell on the p-side were identified as crucial loss channels. Both scale with the active area and, hence, are direclty correlated to the luminescence scaling in active area. As a result, these optical losses partly compensate the potential efficiency gain with increasing area enhancement, as can be seen in Fig. 7. A rate equation model, calibrated on state-of-the-art thin film LEDs and IQE results of the electronic model, was used to describe the IQE droop. We find, that the maximum EQE can be expected at area factors of the order of 10-20. Beyond this, increasing optical losses lead to a significant drop of the extraction efficiency, over-compensating the gain in IQE. Noteworthy, this is almost independent of whether the area enhancement is obtained via a high aspect ratio of the individual NRs or via a dense filling factor of the array of NRs. On the right hand side of Fig. 7, the impact of photonic crystal effects is shown. The highest EQE can be reached if the NR LED is operated in the pseudo-photonic band gap. This is the setup where the horizontal emission of the nano rod in the array (named TM in fig. 3) lies in the band gap and is therefore suppressed.

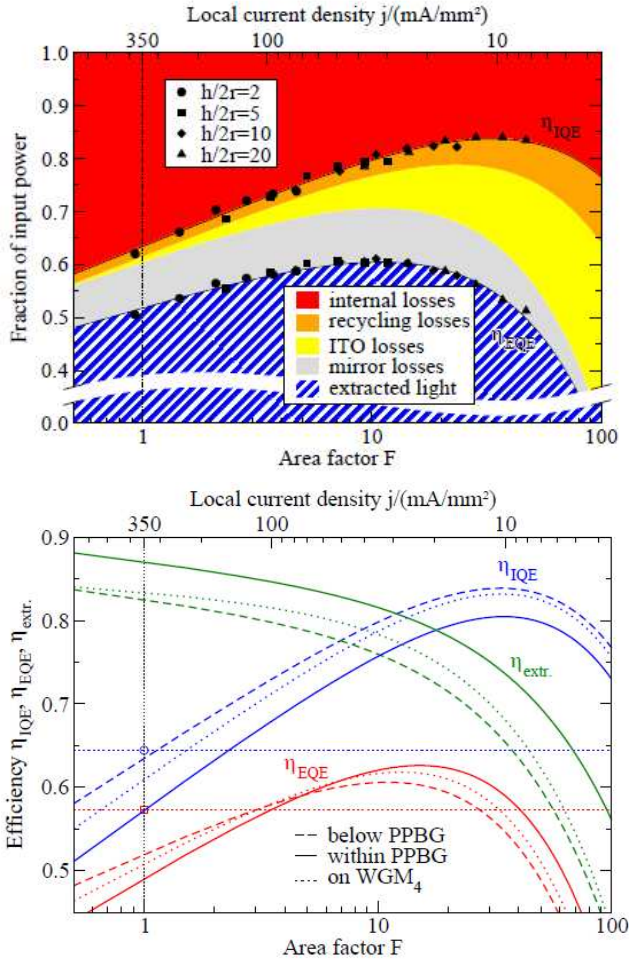

Fig. 7: Loss channel analysis (left) and efficiencies (right) of core-shell NR LEDs as a function of the active area enhancement factor.

Monolithic Phosphorless White Quantum Disc NR LEDs

Applying the multi-color version of the above model, a variety of different, phosphorless white NR LED concepts was investigated. This includes a parallel setup, with individual regimes of blue, green, yellow and red emitting NRs ([B][G][Y][R]) as well as stacks of blue, green, yellow and red emitting QWs within each individual NR ([BGYR]). The wavelengths of the four colors were optimized for highest spectral efficacy at a target color temperature of Tc=3000K and a target color rendering index of Ra=90. Rather than using state-of-the-art internal quantum efficiencies – which would be rather poor at long wavelengths – the spectral drop of the IQE was varied in this analysis. We may thus predict that IQEs of at least 77%, 54%, 40% and 25% at wavelength of 463nm, 529nm, 573nm and 613nm would be needed to achieve a luminous efficacy of 130lm/W. This corresponds to a spectral IQE drop of about -0.3 to -0.4%nm-1. With decreasing filling factor, the maximum allowed IQE drop decreases, as the lack in active area needs to be compensated by higher efficiencies. These values compare to a spectral IQE drop of about -0.7%nm-1 which is typical for state-of-the-art thin film InGaN LEDs.

Workpackage 3:

The overall aim of this workpackage was to establish scalable materials technologies based on nanorod coalescence for achieving low-defect-density and bow-free GaN templates on sapphire and silicon substrates. These technologies were first developed for 2" (50 mm) diameter polar GaN and subsequently extended to semi-polar and non-polar GaN orientations and then transferred to 4" (100 mm) diameter substrates. To meet this goal Work Package 3 (WP3) was divided into the following four main tasks, each of which was successfully fulfilled:

WP3.1 Formation of polar GaN nanorod arrays on 2" (50 mm) diameter sapphire and coalescence into a continuous layer;
WP3.2 Formation of polar GaN nanorod arrays on 2" diameter Si and coalescence into a continuous layer;
WP3.3 Formation and optimisation of non-polar and semi-polar nanorods and coalescence into a continuous layer;
WP3.4 Up-scaling of material growth methodologies to 4" (100 mm) diameter wafers.

The objective of growing fully coalesced GaN epitaxial layers on 50 mm diameter layers (WP3.1) was met early in the project, and wafers were supplied for LED fabrication by Month 6 (M6). The technology, known as nano-pendeo growth, for realizing these coalesced GaN templates was improved via the adoption of nano-imprint lithography (NIL), which enabled highly regular arrays of GaN nanorods to be formed. By M18, average densities of non-radiative defects of $1\text{-}3\times10^{8}$ cm^{-2} measured by cathodoluminescence (CL) across the wafer were achieved in the coalesced layers, compared with edge dislocation densities of 2×10^{8} cm^{-2} measured by x-ray diffraction analysis. By developing a variant of the nano-pendeo growth method in which strategically oriented dashed-shaped, nano-scale mesas (nano-dashes) were used instead of ordered hexagonal arrays of nanorods densities of non-radiative defects as low as 3×10^{7} cm^{-2} were obtained.

In WP3.2 fully coalesced GaN layers with a dislocation density in the order of $8x10^{8}$ cm^{-2} were realized on 50 mm diameter substrates, the thickness of the GaN layers being much thinner than those normally needed in conventional epitaxial growth to achieve such dislocation densities. As a consequence of the accelerating effort in the LED industry to develop LED manufacture on large-area Si substrates, it was decided at M15 that work on developing low-defect density GaN templates would focus on the up-scaling of the nano-pendeo processes to 100 mm (4 inch) sapphire and to Si(111) substrates with a target threading dislocation density of $<5\times10^{8}$ cm^{-2} across the whole wafer. By M36, this target was achieved for both 100 mm diameter sapphire and 100 mm diameter Si substrates. The reduced thickness of the coalesced GaN epitaxy needed to achieve such dislocation densities offers a real advantage in the manufacture of light emitting diodes (LEDs) with the prospect that further optimization of the nano-pendeo technique, for example using the nano-dash approach, will further reduce the dislocation density.

In WP3.3 processes for growing epitaxial non-polar (11-20) and semi-polar (11-22) GaN templates, by coalescing "bottom-up" GaN nanorods grown by molecular beam epitaxy (MBE) along these crystallographic directions, were developed. The process involved first growing non-polar and semi-polar GaN templates by metallorganic vapour phase epitaxy (MOVPE) and then by growing the nanorods, from these templates by MBE via a growth mask (selective area epitaxy - SAG). The starting templates were known to contain very high densities of partial dislocations and stacking faults which are known to compromise the luminescence of the material by introducing a high number of non-radiative recombination centres. Therefore, photoluminescence (PL) was used to assess the quality of the non-polar and semi-polar layers grown by the bottom-up approach. In the case of both non-polar and semi-polar

materials, the PL intensity of the overgrown layer was much larger than that of the initial template. Furthermore, the PL of the final templates at room temperature is dominated by band-edge emission while at low temperature it is dominated by donor-bound emission. Moreover, the emission from stacking faults in the final coalesced template is at least a factor 5 smaller than in the initial one. These emission features point towards an effective reduction of structural defects in such non-polar and semi-polar templates. This innovation represents a break-through in growing non-polar and semi-polar GaN templates, an area of increasing technological importance notably for manufacturing green and yellow LEDs.

Finally, in WP3.4 successful up-scaling of the nanopendeo growth technique on both 100 mm diameter sapphire and 100 mm diameter Si substrates was demonstrated with excellent homogeneity across the full wafer. The coalesced layers obtained using optimized growth conditions and optimized pattern geometry were shown to have a low surface roughness (typically below 1nm), to be crack-free, and displaying a dislocation density systematically below $5\times10^{8}cm^{-2}$, for both Sapphire and Silicon substrates. Thanks to these characteristics, the coalesced templates on silicon perfectly meet the industrial requirement of LED production. Several 100mm templates have been provided to OSRAM for LED fabrication using their production line. A first demonstrator on sapphire was obtained at M24 while the fabrication of a demonstrator on silicon substrate was in progress at the time of writing this report.

Highlights of WP3.1

Two nano-pendeo processes were developed based on etching a regular nanostructure into the surface of a pre-existing GaN template, in the case of WP3.1 grown on 50 mm diameter sapphire substrates. Both processes involve further MOVPE growth which initially results in the formation of GaN nano-pyramids which are then, with a change of growth conditions, coalesced into a continuous film. Thereafter, the processes diverge. U Bath uses a pulsed growth technique to overcome the self-limiting growth process by which the nano-pyramids form, to promote lateral growth from the side facets of the nanopyramids until they touch and coalesce. The CNRS-CRHEA process involves perturbing the self-limiting growth process without having to pulse the reagent flow in order to achieve lateral growth of the nano-pyramids and their ultimate coalescence. Figure 1 compares the early phase of coalescence by the CNRS-CRHEA technique (a) and (b) and by the U Bath technique (c). The U Bath approach involves using a pulsed MOVPE growth mode which enables rapid lateral growth but has the disadvantage that inevitable inhomogeneity in the nanopyramids gives rise to local differences in the rate of coalescence, causing island growth to occur. The distribution of dislocations in subsequently fully coalesced films can then reflect this island structure. On the other hand, while in the CRHEA-CNRS approach the lateral growth is smaller, the coalescence process is completely homogeneous.

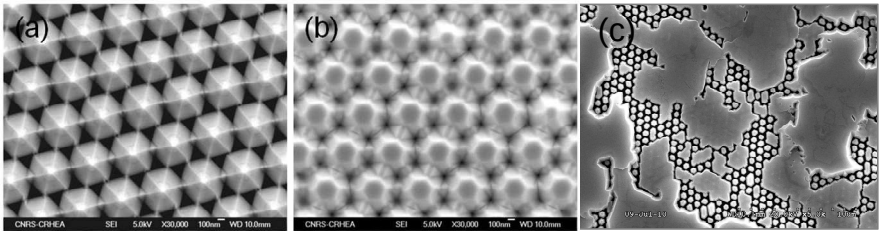

Figure 1 Comparison of the early stage of MOVPE growth of nanopyramids and their expansion (a) at the start of coalescence and (b) part way through coalescence by the CNRS-CRHEA technique with the U Bath approach (c) also at an early stage of coalescence.

A systematic study of the impact of the coalescence growth conditions on the quality of the resulting continuous epitaxial GaN films enabled the identification of conditions that reduced the density of edge dislocations in the coalesced GaN films. Table 1 summarizes some of the results of this study which resulted in typical maximum total dislocation densities of around 3-4x10^8 cm^{-2}, a result improved in coalesced GaN films formed on 100 mm diameter sapphire substrates (see section 4 below).

Pyramids growth duration	X-ray (002) FWHM (°)	X-ray (302) FWHM (°)	AFM Screw DD (cm^{-2})	AFM Edge DD (cm^{-2})	AFM Total DD (cm^{-2})	DD Screw/Edge ratio	RT-PL Band-edge energy (eV)
1400sec	0.086	0.155	2.4x10^8	3.1x10^8	5.5x10^8	0.77	3.4226
2000sec	0.077	0.149	1.8x10^8	1.8x10^8	3.6x10^8	1	3.4244
2400sec	0.077	0.158	2x10^8	5x10^8	7x10^8	0.40	3.4215

Table 2 Rocking-curve values of the (0002) and (30-32) reflections, dislocation densities and room-temperature band-edge emission energy on coalesced GaN templates at CNRS-CRHEA as a function of the pyramid growth duration.

A new nano-pendeo process consisting of coalescing GaN grown from nanodashes rather than circular nanorods was developed. Fast lateral expansion can occur on strategically aligned nanodashes without creating structures that are bounded by slow-growing *r*-plane facets to avoid downward growth in the *-c* direction which had been shown to be a significant cause for the incorporation of new dislocations in the coalesced layer. Figure 2 (a) and (b) show SEM images of two nanodash patterns formed by NIL and inductively coupled plasma etching prior to growing the nanopyramids. Figure 2(c) shows a partially coalesced GaN film resulting from expanding the elongated nanopyramids and Figure 2(d) shows a fully coalesced, planar GaN epitaxial layer formed by this process.

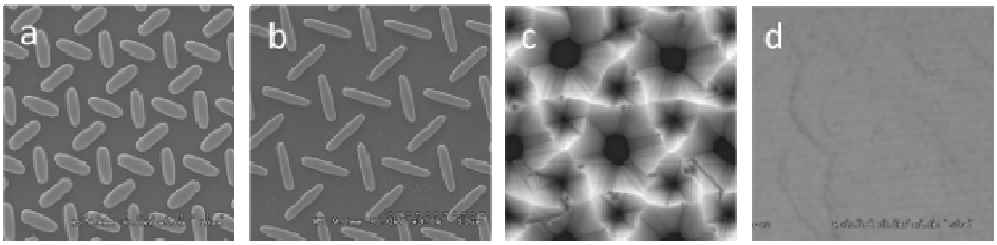

Figure 2 a) and b) SEM images of two regions of nanodash template prior to regrowth. c) First growth stage from nanodashes, and d) SEM image after planarization.

Cathodoluminescence (CL) was used to determine the density of non-radiative recombination centres in the resulting coalesced films. It was found that the average CL dark spot density in coalesced layer initiated from nanodashes with an aspect ratio of ~15 was estimated at 3x$10^7$$cm^{-2}$ with areas approximated 5x5μm in extent where the CL dark spot density was as low as 4x$10^6$$cm^{-2}$. Note that layers in which these low densities of non-radiative recombination centres were observed were very thin.

Highlights of WP3.2

After completing preliminary work on forming fully coalesced GaN layers on 50 mm diameter Si substrates with threading dislocation densities of around 8×10^8 cm^{-2} by M15, the decision to accelerate the up-scaling work resulted in the achievement at M18 of fully coalesced GaN layers on 100 mm diameter Si

substrates with very similar defect densities. As a consequence, the development of optimum nano-pendeo processes that resulted in crack-free coalesced layers with low dislocation densities (< 5×10^{8} cm^{-2}) low surface roughness (< 1 nm) and reduced wafer bow on 100 diameter Si substrates became the new focus of this task.

Careful optimisation of the nanorod pitch, height and passivation, along with the identification of the optimum orientation of the nanopyramids resulted in spectacularly uniform coalescence with almost fully planarized GaN layers after growing a film of just 500 nm thickness, see Figure 3. Estimates of the screw and edge dislocation densities, obtained from high resolution X-ray reflection measurements performed systematically across the 100 mm diameter wafer, revealed that the dislocation density was uniformly distributed between 4-$5\times10^{8}cm^{-2}$. These results are more fully described in section 4 below

Highlights of WP3.3

In performing the work of this activity UPM accomplished the selective area growth of non-polar [11-20] GaN nanorods by MBE on top of non-polar GaN templates. To our knowledge, this is the first time that such a growth (i.e. non-polar, axial GaN nanorods by MBE) has been ever reported, and it constitutes the first step towards the fabrication of coalesced non-polar templates by a fully bottom-up approach. Figure 3 shows examples of these non-polar nanostructures after optimization of the growth conditions, a perfect selectivity, similar to the one obtained on c-oriented samples, has been achieved. Compared to the most common hexagonal *c*-oriented NRs, the non-polar ones show an elongated morphology along the <0001> direction, which in this case is parallel to the substrate surface. Figure 4 shows the results of a sample formed after a longer growth time, which resulted in almost full coalescence, to identify a very promising way to obtain high quality, low dislocation non-polar GaN films (overgrown by MOVPE) on non polar GaN templates of much lower quality.

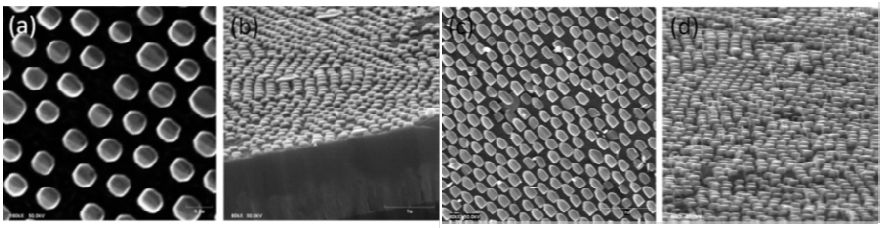

Figure 3 SEM images of non-polar GaN NRs obtained by plasma-enhanced MBE on non-polar GaN templates grown by MOVPE: (a) top and (b) side views of GaN NRs obtained under an equivalent N flux of 5nm/min; (c) top and (d) side views of GaN NRs obtained under an equivalent N flux of 10nm/min.

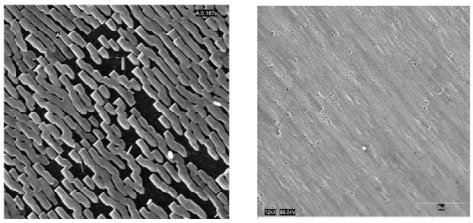

Figure 4 SEM images of non-polar GaN NRs grown on a-plane GaN realized with a longer growth time. Coalescence along stripes in the (0001) direction is clearly observed.

PL measurements verified that the non-polar GaN nanorods and nearly coalesced layer shown in Figure 4 were of significantly higher quality than the starting *a*-plane templates, see Figure 5. The PL

obtained from the *a*-plane GaN template shows a very weak band edge emission and broad yellow emission. However, the GaN nanorods grown on this type of template show a narrow band edge emission and no presence of yellow band, indicative of a high crystal quality. The results about ordered GaN growth on a-plane templates (grown by MOVPE at CNRS-CRHEA) by UPM were published in *Journal of Crystal Growth* Volume 353, Issue 1, Pages 1-4, 2012.

A similar process was developed for semi-polar (10-22) GaN, see Figure 6. Figure 7 compares the low temperature (12 K) photoluminescence spectra of the semi-polar starting template and the selective ordered growth on top, demonstrating the significant improvement in the optical quality of the material by a higher intensity and lower full width half maximum.

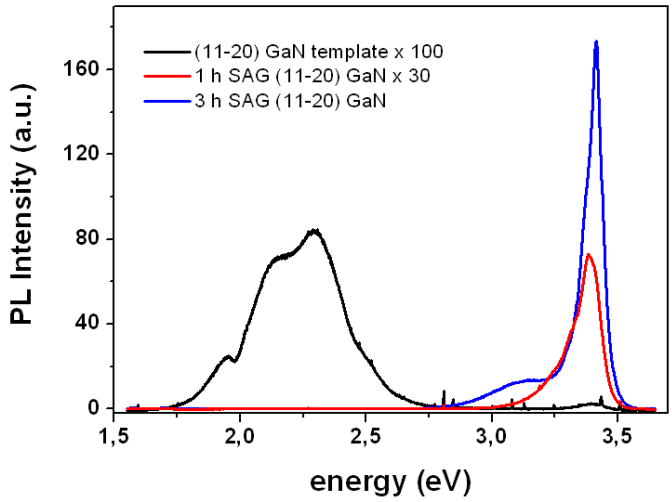

Figure 5 Room temperature spectra of: a-plane GaN template (black), 1-hour growth GaN nanorods on a-plane GaN (red) and 3-hours growth GaN nanorod on a-plane GaN (blue).

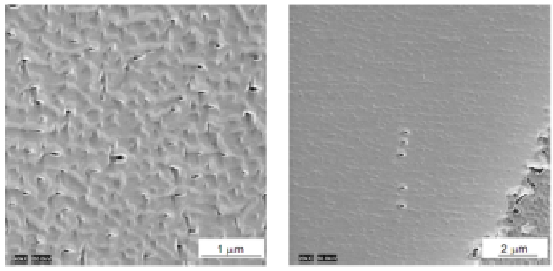

Figure 6 SEM images of partially coalesced areas after 3 hours of GaN selective growth on semi-polar templates.

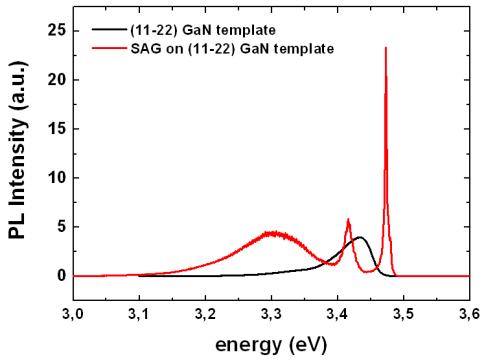

Figure 7 Low temperature photoluminescence of a semi-polar GaN template (black line) and after selective area growth (SAG) on top of the template (red line).

Highlights of WP3.4

The milestone of up-scaling each of these processes and their incorporation into a reliable wafer flow was reached by M18, twelve months ahead of schedule (Milestone M3.5 due in M30 in the original Description of Work). This resulted from the developments in GaN nanorod fabrication that UoB were able to achieve in the period M12-M18. The perfect homogeneity over the entire 100 mm wafer was quantitatively characterized by scanning electron microscopy (SEM). The height and the diameter of nanorods were measured by SEM and a deviation of less than 10% was found from the wafer center to the wafer edge, thereby confirming the suitability for subsequent coalescence, Figure 8. This precision in nanorod generation was matched by (100 mm diameter) wafer-scale uniformity that CNRS-CRHEA were able to achieve in first growing and then expanding the {0-11} faceted GaN nanopyramids on the tips of the nanorods, see Figure 9.

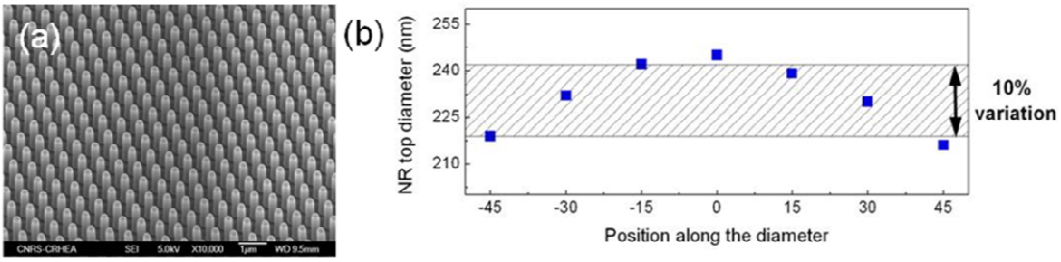

Figure 8 Tilted SEM image of GaN nanorods on 100 mm wafers (a), and nanorod diameter as a function of the position on the 100 mm wafer.

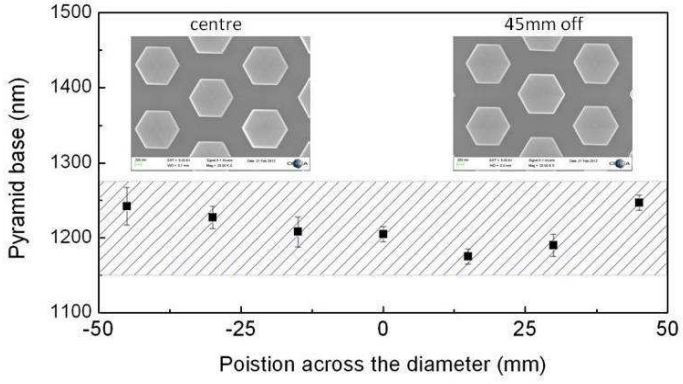

Fig. 9 Pyramid size as a function of its position across the passivated 100 mm substrate.

In a refinement of the nanorod generation process designed to eliminate a problem experienced of intermittent parasitic growth experienced by CNRS-CRHEA, LETI developed an alternative method of passivating the nanorod sidewalls and space in between, see Figure 10(a). By combining the nanorods treatment optimized at UoB, the LETI passivation and the new pyramid growth conditions for passivated templates developed at CNRS-CRHEA, homogeneous pyramid formation was obtained, Figure 10(b). On nanorod templates with larger pitch size, which should in principle allow further dislocation reduction, AFM measurements on partially coalesced templates have shown areas with dislocation density as low as $1\text{-}2\times10^{8}\text{cm}^{-2}$.

Since the optimizations on sapphire highlighted the fact that the final dislocation density is strongly dependent on the switching from the pyramid growth step to the enhanced lateral growth conditions, the same study has been performed on silicon. Once again, the coalescence has been completed by the growth of a 500nm thick GaN layer. All three templates present a fully coalesced surface without any un-coalesced areas and their X-ray diffraction rocking curves are quite similar, with full width at half maximum of 0.150° for the (002) reflection and 0.190° for the (302). The linewidth values, especially for the (102) and (201) reflections, of the coalesced templates represent a large improvement compared to those of the initial GaN templates provided by OSRAM. Measurements of the dislocation density by the AFM technique indicate that the screw dislocation density is as low as $2\text{-}3\times10^{8}$ cm^{-2}, which is comparable to the best coalesced template on sapphire.

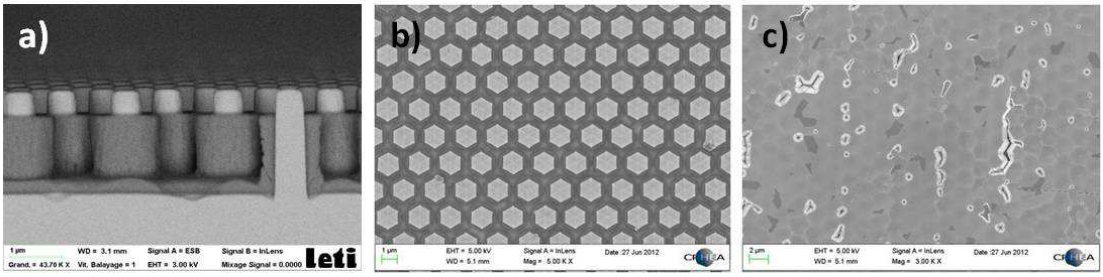

Figure 10 2000nm pitch nanorod template passivated at LETI (a), after pyramids growth (by MOVPE at CNRS- CRHEA (b), and after partial coalescence process (c).

One difference with the optimized nano-pendeo process for coalescence growth on sapphire was the need grow an AlN layer during the coalescence to prevent cracking, a technique commonly used in conventional methods for growing planar GaN on Si. Preliminary results show that the addition of a thin AlN layer allows the growth of crack-free 750nm thick coalesced GaN films. Room-temperature photoluminescence measurements clearly show that the two coalesced templates with AlN inter-layers are either strain-free or present a residual but beneficial compressive strain, while the cracked template grown without the AlN inter-layers is under tensile strain.

In summary, by meeting the milestones and deliverables redefined at the M18 review, a manufacturing technology for fabricating 100 mm diameter *c*-plane GaN templates by the nano-pendeo technique has been researched and developed. The best 100 mm diameter ~500 nm thick templates had threading dislocation densities in the range $2\text{-}3\times10^{8}$ cm^{-2} irrespective of the substrate type (sapphire or Si) used. Achieving such low densities of threading dislocations in such thin GaN, large diameter layers represents a significant advance in the state of the art of the nano-pendeo method. Preliminary work on extension of

the method to nano-dash rather than rod-shaped nanostructures has been found to offer interesting possibilities for substantial further reductions in the density of threading defects in coalesced GaN layers.

In an innovative extension to the nano-pendeo technique, a combined MBE-MOVPE method for growing coalesced non-polar and semi-polar epitaxial films has been developed. The new method involves growing non-polar and semi-polar nanorod by MBE and then coalescing them using MOVPE. The GaN band edge photoluminescence of the SAG material is much more intense and has a significantly narrower linewidth than the underling template and shows far less defect band luminescence.

Workpackage 4:

Workpackage 4 had two different lines of work dedicated both towards the achievement of nanoemitters. The first line focused on the selective area growth (SAG) by MBE of III-Nitrides nanorods and the second one on the growth by MOCVD of ordered coreshell structures. In both cases, the final objective was to use these ordered structures to fabricate arrays of nanoLEDs with broad emission.

For the first line of work (i.e. MBE growth of ordered nanorods) the main highlight has been the achievement of of SAG by MBE of III-N nanorods ensembles with controlled size, height and density necessary for subsequent Nano-LED fabrication (height & diameter dispersion < 20%) using Ti-masked GaN templates.

The SAG process is critically affected by the roughness of the Ti-mask and also the different MBE growth parameters such as substrate temperature and N/Ga fluxes ratio. Figure 1 shows the effect on selectivity by increasing the growth temperature (from 940 to 960ºC) in three different samples grown on the same type of mask and with the same N/Ga ratio. As the growth temperature is increased, the desorption of Ga atoms from the surface of the mask is enhanced leading to better selectivity, but growth rate falls down. Growths performed above 960ºC result in the complete desorption of all the Ga, with no growth at all. Once the optimal substrate temperature was determined, different analysis were also performed to study the effect of the III/V ratio. It is found that for a specific growth temperature (always below 960ºC) and mask geometry (i.e. dimensions of the hole diameter and pitch), the III/V ratio needs to be adjusted properly in order to preserve the selectivity and enhanced the ordered growth within the nanoholes.

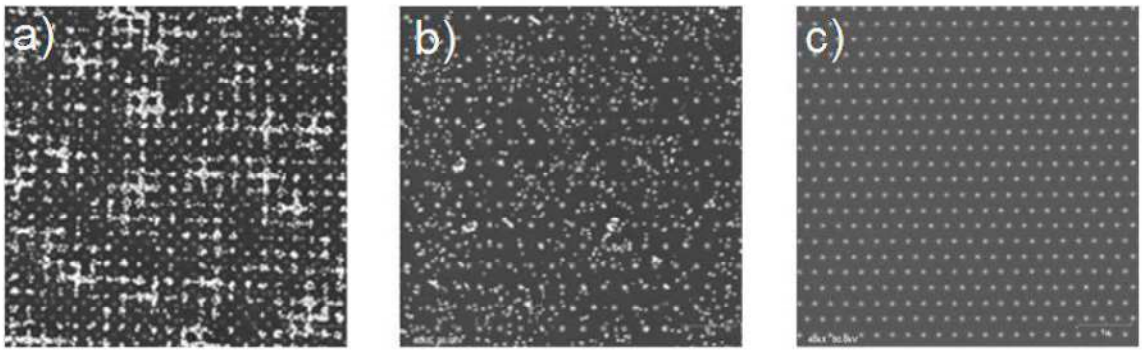

Figure 1 -. SEM pictures of three samples grown at UPM with the same Ga (10 nm/min) and N (15 nm/min) fluxes but increasing growth temperature: (a) 940ºC, (b) 950ºC and (c) 960ºC

Following the optimization process, both deliverable D4.1 (“Prototypes of ordered nanorod ensambles”) and milestone M4.1 (“Nanorod ensembles with controlled size, height and density necessary for subsequent Nano-LED fabrication; height & diameter dispersion < 20%”) were achieved and reported (see reports on D4.1 and M4.1). Summary of the results obtained in these targets are summarized in Figure 2.

TUBS has also achieved SAG of ordered GaN nanorods on patterned SiO2/sapphire templates with aspect ratios in a range of 2-8 using their own templates depending on the pattern. TUBS has also investigated the influence of the different growth parameters (i.e. III/V ratio, reactor pressure and total carrier flow) on the GaN nanorod morphology and selectivity. In general, it is found that the polarity in combination with hydrogen carrier gas are crucial parameters to have GaN nanorod growth. The SEM picture of Figure 3 represents a typical sample once all these optimization processes have been applied and shows the statistics on the dispersion of diameter and height values obtained, fulfilling both the deliverable D4.1 and milestone M4.1.

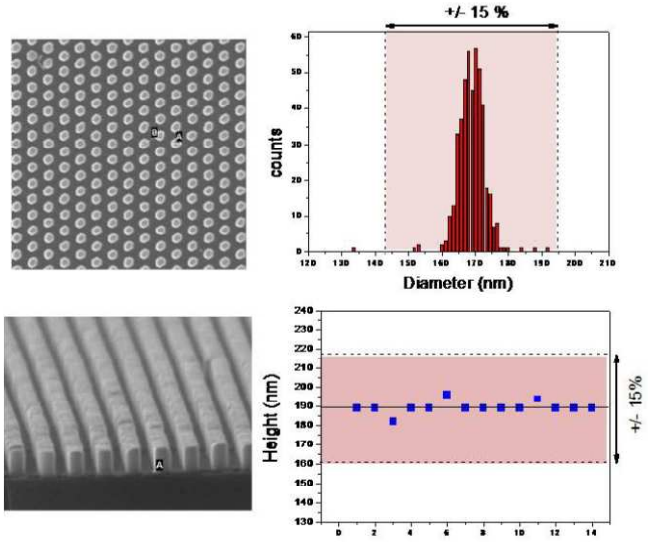

Figure 2 - SEM pictures of GaN nanorods grown by MBE at UPM on Ti-masked GaN with holes of 170 nm diameter. Dispersion of diameter and height values fulfilling specifications of milestone M4.1

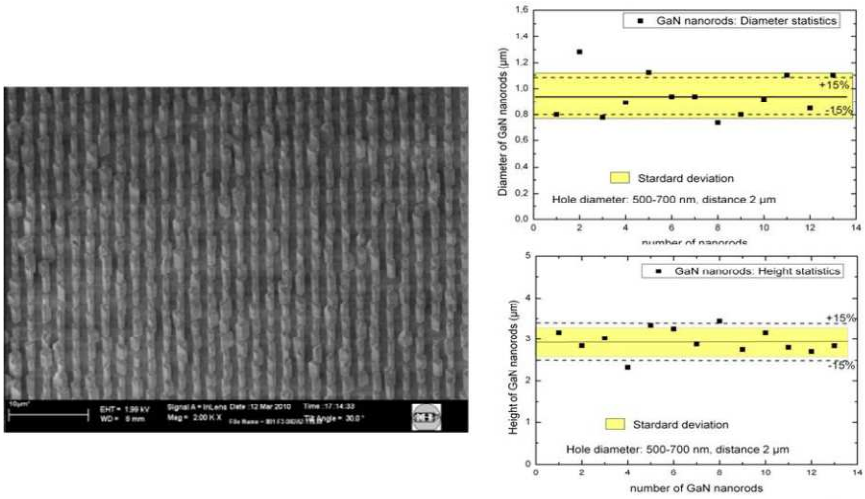

Figure 3 - SEM image of GaN nanorods grown by MOCVD at TUBS on a pattern with a diameter of D 500-700 nm and a distance of;2 µm. Dispersion of diameter and height values fulfilling specifications of milestone M4.1

Another highlight within this WP is related with growth of emitting structures. UPM has demonstrated the possibility of fabricating different structures with controlled emitting wavelength using various approaches. One of these approaches consisted in growing InGaN nanorods sections on top of ordered GaN nanorods. The InGaN section could be grown either at a fixed growth temperature (leading to a nominally constant In composition and therefore a single colour emission), or modifying the substrate temperature during the growth of the InGaN nanorod (without modifying the Ga, In and nitrogen supply) as to produce an InGaN nanorod with a composition gradient along the growth axis. In the first approach, by tuning the growth conditions (i.e. substrate temperature and III/V ratio) during the growth of the InGaN section, it was possible to achieve PL emission at the three primary colours. Figure 4 shows the room temperature PL spectra and photographs of the real colour obtained for each sample.

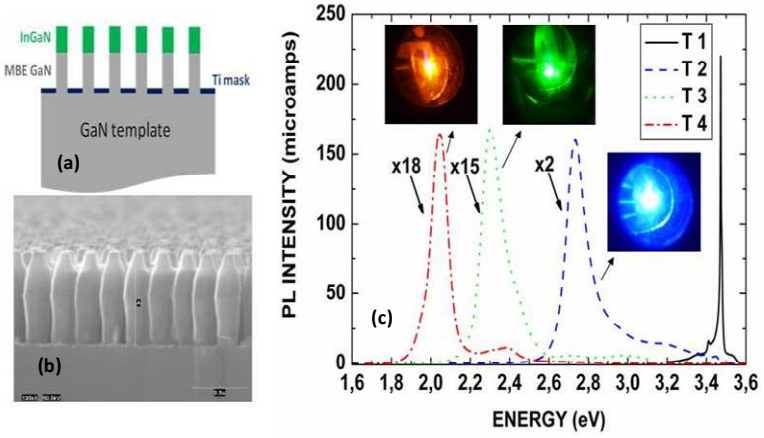

Figure 4. (a) Schematic of the grown ordered nanostructures with fixed In composition in the InGaN section. (b) typical SEM photographs of the ordered nanostructures, and (c) room temperature PL spectra and photographs of samples with 40% (T4), 29% (T3), 18% (T2) and 0% (T1) of In.

For the second approach, the substrate temperature was varied from 750º to 625 ºC, which should lead to a lower In composition in the lower part of the InGaN section (higher growth temperature implies higher In desorption and therefore lower In incorporation, blue color) and a higher In composition in the top part of the InGaN section (red color). The combination of these different sections should give a broad emission which is needed for a white light emitter. Figure 5 shows low and room temperature PL spectra of an optimized graded sample (with three thin GaN barriers along the InGaN section). Low temperature CL characterization of a single nanorod has also been performed and the result is also provided in Figure 5, showing clearly the different emissions coming from the different sections of the InGaN nanorod.

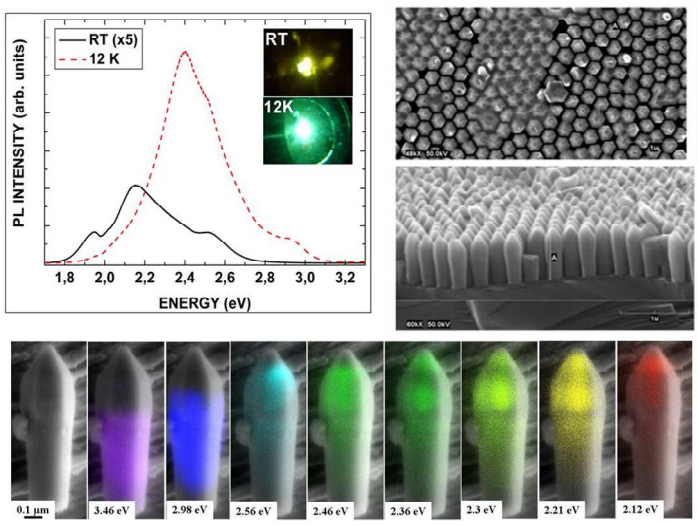

Figure 5. Low temperature PL spectrum, real-color photograph, SEM pictures of the ordered sample grown with a In composition gradient along the growth axis, and low temperature CL images at different energies of a single InGaN/GaN nanorod grown with a gradient composition along the growth axis.

A second approach employed to obtain broad emission was to combine the results obtained separately in Task 4.2 (growth of nanorod emitters with controlled colour). In that Task it was demonstrated that the three primary colors could be obtained by growing ordered InGaN nanorods with different compositions (Figure 4). The current approach would combine three different InGaN sections (with different In composition, x1<x2<x3) grown one on top of the previous one within the same nanorod structure (named RGB sample). Figure 6 shows a schematic, SEM photograph as well as the room and low temperature PL spectrum of a sample grown with 3 different InGaN sections, each one with an Indium composition of 18, 29 and 40 %. The thickness of each InGaN section was determined and modified in several experiments taking into account the weight of each color within the spectrum of white light and normalizing the PL spectra obtained from each individual emitter (Figure 4). The PL emission obtained in the optimized structure (figure 6) is also a broad one and the color obtained is almost a perfect white.

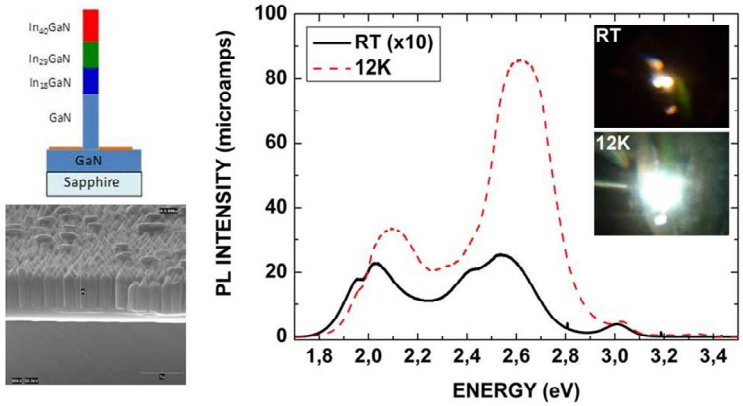

Figure 6. Schematic, SEM image and room and low temperature PL (with real-color photograph) of a RGB ordered sample, using three InGaN sections with different In composition/ thicknesses.

With all the previous results, InGaN-based p-i-n nanorods were designed and grown keeping a columnar structure and preserving selectivity during the initial Si-doping stage (i.e. bottom part of the nanorod). All p-i-n structures presented in this WP were grown with a bottom Si-doped GaN n-type section and a top Mg-doped GaN one (Figures 7 and 8).

The SEM photographs of figure 7 reveal that the ordered growth is successfully achieved and the coalescence of the nanorods is avoided, although an increase of the diameter on the top section of the nanorod is observed, especially for the two samples grown at a lower substrate temperature (b and c).

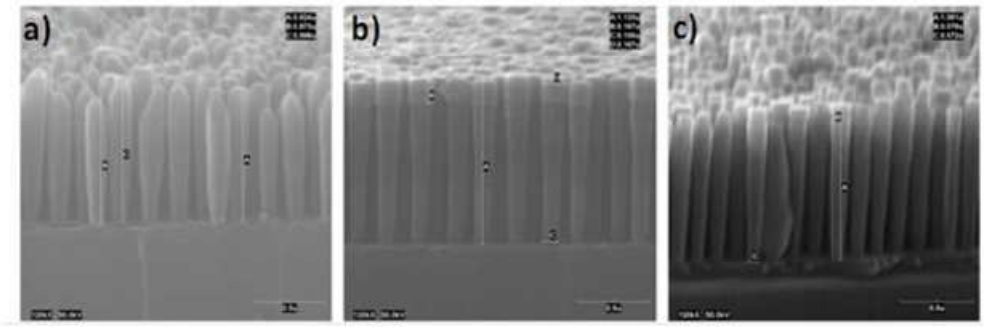

Figure 7. Cross section SEM photographs of p-i-n structures with different InGaN intrinsic regions. (a) InGaN grown at 700ºC, (b) InGaN grown at 650º C and (c) InGaN grown varying the growth temperature from 720º to 600º C (graded In composition).

Figure 8 shows the room temperature PL spectra of the p-i-n samples already described. A single emission can be observed for the case of the two structures with the InGaN section grown at a fixed substrate temperature (i.e. single colors, centered in the blue and green respectively). However, a broader emission (whitish) is observed for the third sample with an InGaN section with a gradient In composition. The IQE values obtained from these samples are quite high for the first two with fixed In composition (between 60 and 70%). For the case of the broad emission sample, accurate IQE values cannot be provided at this time due to limitations in the PL set-up.

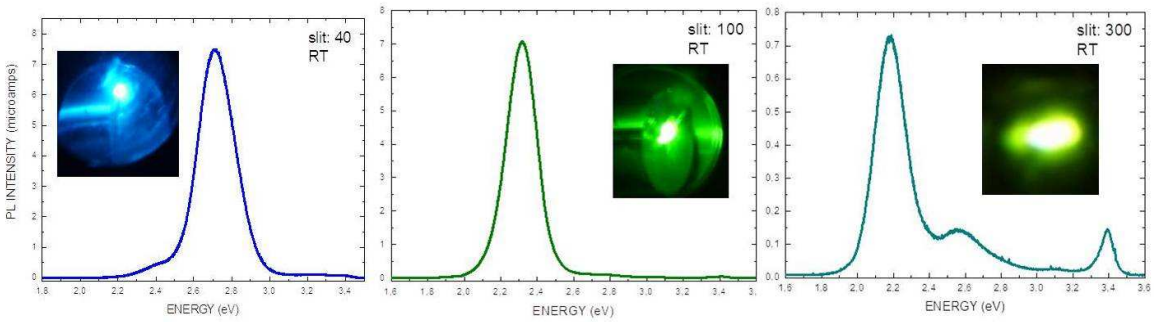

Figure 8. Room temperature PL spectra and real-color photographs of the p-i-n structures shown in Figure 7.

For the case of the growth and fabrication of nanoLEDs based on coreshell structures, the results obtained by TUBs include also significant highlights.

N-polar and Ga-polar 3D GaN columns have been realized on patterned SiO2/sapphire templates fabricated by photo lithography and on patterned SiO2/GaN/sapphire O3 templates (nano imprint lithography) by MOVPE, respectively. In particular, it is found that the V/III ratio and SiH4 flow are key parameters of Ga-polar nanorod growth on conductive templates. High quality nanorods with an aspect ratio of 20 have been achieved.

The core-shell geometry of InGaN/GaN MQWs and p-GaN has been realized on N-polar and Ga-polar n-GaN columns. TEM images of single rods prepared by FIB in plan view geometry (Figure 9) clearly show that both the MQW and the p-GaN completely cover the n-doped GaN rod.

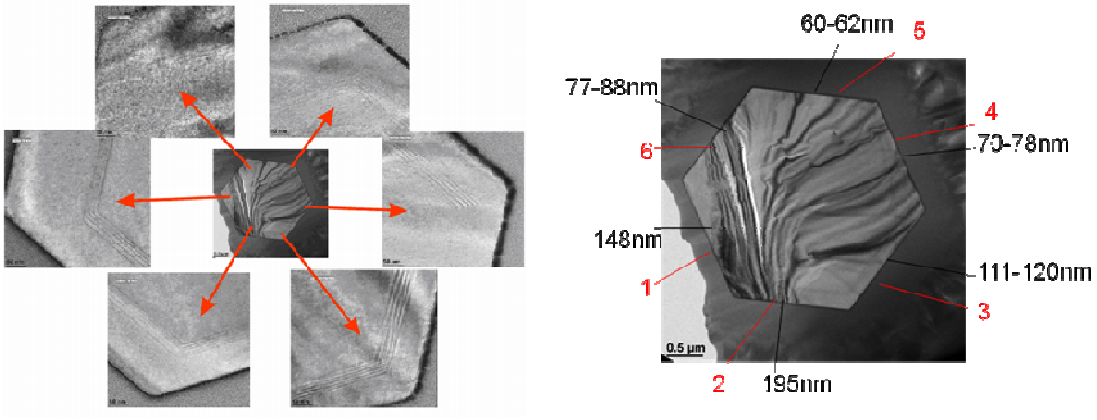

Figure 9. Plan view TEM image of a core-shell rod LED (centre) with enlarged images of each corner showing the fivefold MQW and p-GaN on the m-planes; right part: TEM plan view with indicated p-GaN thicknesses on each m-plane facet.

Room temperature cathodo luminescence (RT CL) was used to control the spatially resolved optical quality of the core-shell LED structures. Figure 10 shows a typical spectrum (left). From the superimposed images (right) it becomes clear that the 400 nm peak has its origin on the m-planes whereas the lower intensity peak at 470 nm wavelength originates on the top c-facet. The missing yellow band emission around 550 nm demonstrates the high crystal quality of the rods. With these results, Milestone 4.3.A (i.e. " Three high quality quantum wells achieved in core shell type structures") was successfully achieved.

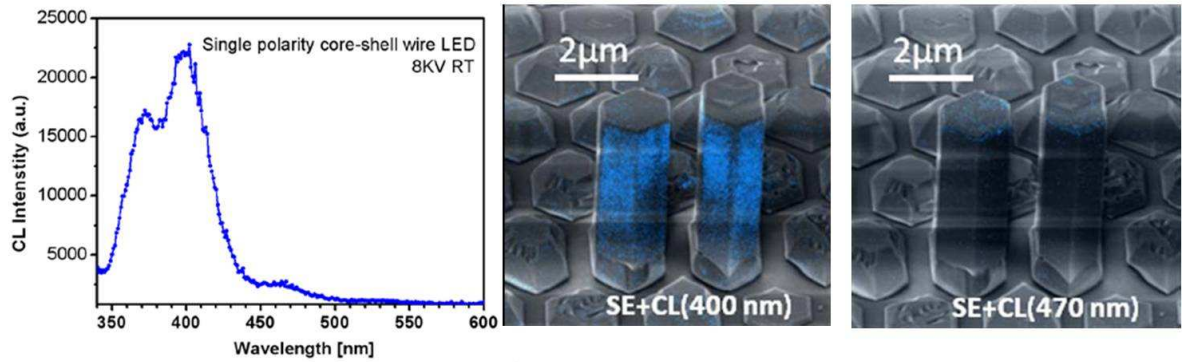

Figure 10. RT CL spectrum of core-shell LED rods taken at 8kV (left); corresponding secondary electron images superimposed with CL images taken at peak wavelengths of 400 nm and 470 nm.

Dislocation-free high aspect ratio Ga-polar GaN nanorod arrays have also been achieved by MOCVD on patterned SiO2/GaN/sapphire conductive templates. Core-shell LED structures

have been grown on these nanorod arrays, the geometry has been proved by CL measurements.

Room temperature (RT) cathodoluminescence (CL) spectra of Ga-polar GaN coreshell LEDs are shown in Figure 11. The CL monochromatic intensity maps were taken at a wavelength of 400 nm using an acceleration voltage of 5 kV. At this wavelength, the MQW emission from the m-planes is clearly visible and no emission was observed from r-planes.

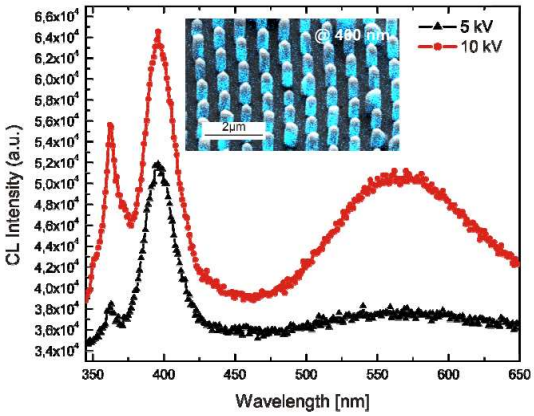

Figure 11. Normalized CL spectra at room temperature with an acceleration voltage of 5 kV and 10kV, respectively; these spectra are vertically shifted for clarity. Inset: colour-coded RT CL maps at 400 nm wavelength superimposed on FESEM images of Ga-polar nanorod core-shell LEDs.

Finally, SEM image analyses show an increase of active area in ensembles of core-shell LED structures of a factor of up to 5.5 when compared to LEDs of the same geometry but with an active region only on the top facet. (Milestone 4.6). Scanning electron microscopy (SEM) and surface profiling were used to analyse the geometry of the grown structures. Figure 12 shows a secondary electron image of a part of an array with nominal diameter and pitch of the rods of 400 nm and 4 µm, respectively. The geometrical dimensions of all analysed LED rods are collected (right). The data points above the black line possess an increased active area by at least a factor of 5 when compared to conventional nano-LEDs with the respective diameter.

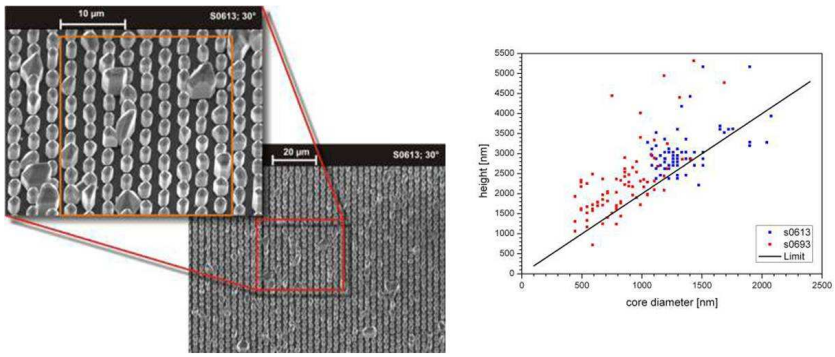

Figure 12 . (Left) SEM images of a core-shell rod LED ensemble selectively grown by MOVPE through a SiO_2 mask with nominal openings of 400 nm and a pitch of 4 µm. In the enlarged image the rectangle marks the analysed area.. (right) Measured height and core diameter of the analysed 155 rods of two different samples. The black line shows the lower limit of increased active area by a factor of 5 when compared to conventional nano-LEDs of the respective diameter.

Workpackage 5:

In this workpackage multiple tasks have been addressed. Solutions were achieved for frontend and backend processes related to the initial parts and the final parts of the LED fabrication value chain.

Continuous supply of WP3 and WP4 partners with structured substrates was based on process development and provided technology. Optimization of imprint processes as well as etch processes and equipment helped to improve the quality of samples distributed to other project partners.

Especially, the template supply for WP3 was significantly highest priority since the number of necessary templates was significantly increased throughout the project. Respective deliverables have been met during the time period. However, the support for nanoemitter template fabrication within WP4 is mentioned and acknowledged, here.

Major achievements are the prototype of LED on nanorod sapphire template with efficacy > 100 lm/W) and the subsequent optimized growth combined with an upscaling from 2” to 4inch on sapphire. Following the industrial trend for upscaling, consequently the focus was shifted to GaN-on-Silicon substrates to explore the potential of the passive nanorod approach. Therefore various pattern and arrangement of the pattern with respect to the crystal facets were investigated. A point-to-point arrangement of the pyramids grown on top of the nanorods yields the best crystalline quality (lowest density of threading dislocations) for the coalesced layers.

The chip process for overgrown silicon templates was started but not finished until the end of the project, hence any demonstrators showing >150lm/W on silicon could not be shown, yet. The chip processing is ongoing and the results will be communicated along with the demonstrators.

Processing the LED chips out of the nanoemitter and PNR epi material provided from WP3 and WP4 partners has been the second major tasks within this workpackage. Therefore, several approaches for filling, planarization and contacting of nanorod arrays could be demonstrated and evaluated. Additionally, an electrical evaluation of p-contact behavior during exposure was performed. Although the limited number of suitable nanorod material for the chip process development, feasible processes for both, nanoemitter and passive nanorods, have been obtained. White light LEDs have been derived and electro-optical data were analyzed to characterize the performance of the novel nanorod-based material.

The feasibility of the envisioned thin film chip process for active emitter nanorod arrays could be demonstrated using self-assembled nanorods grown on silicon. However, due to lack of samples the LED chip fabrication on grown nanoemitter structures in all colors and phosphor-less white was started late and has not been finished by the end of the project. The work towards meeting all project goals will be continued and the respective results will be reported accordingly even though belated.

Processes for the nanorod template fabrication

Precision nanoimprint and low cost nano replication with disposable master technology have been applied to fabricate templates for position controlled nanorods.

A number of different stamps have been produced and used for imprints during the time period. Stamps with various patterns and dimensions have been produced and used for imprints. In order to use each of these stamps, a Ni plating process is needed followed by antisticking treatment. For imprinting with each new stamp, a process optimization phase was required. In sum, more than 400 wafers have been imprinted and delivered between M1 – M36.

The nanoimprint lithography patterns that have been used in the project have varied from very small patterns (100 nm holes / 200 nm pitch as used in stamp O4) to larger patterns (500 nm holes, 2000 nm pitch as used in stamp M2). The different sizes used in the stamps have required process development and optimization. In particular, nanoimprint lithography on III / V substrates and templates such as these used in the project (i. e. GaN on silicon) is very challenging due to the native roughness of the top surface. A significant amount of work was put into this early in the project to overcome these issues as well as to develop a new stamp replication process (i. e. going from expensive silicon master to multiple nickel copies in order to enable economically feasible manufacturing of nanostructured templates). These two efforts gave significant input to two publications.

In addition, various project partners have been using different tools for their template and epilayer processing which in some cases have required special attention. An example of this is the MOVPE systems used by OSRAM and the MBE systems used by UPM. A significant effort have also been put into producing a large number of samples as was required by WP3 activities and by project partner OSRAM, who needs to use their production equipment for processing in the SMASH project. This means that all samples had to be entire 4” wafers and that each batch normally consists of 25 samples. The major part of these samples have been GaN on Silicon samples, however, there have also been a few samples with GaN on sapphire with SiO2, SiN or Ti as etch mask.

The other nanoimprint technology was mainly applied to the passive nanorod template fabrication. Here, several combinations of patterns and polarities of the shims (positive and negative) have been used. For the coating, disposable master laquer were used and also provided for experiments at UoB along with additional resist for imprinting. E.g., the negative masters (pillars) were imprinted using 16% Autotex III lacquer in ethyl lactate successfully with standard conditions giving a near zero residual layer as shown in the Fig. 5.1 below.

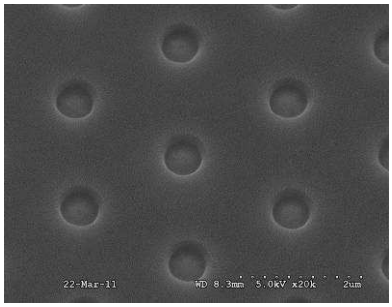

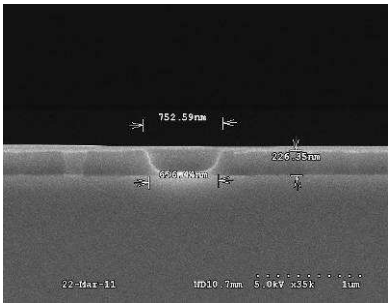

Figure 5.1. Positive 2 micron pitch imprint using 16% Autotex in ethyl lactate spun at 4000 rpm, soft baked for 3 mins at 150 ℃, imprinted from negative disposable master and UV cured for 2 mins. Left: top view. Right: cross-section.

In the last 18 months, experiments have been undertaken to achieve an imprint quality that allows the growth on 4 wafer. In particular, for the GaN-on-Silicon templates, the requirements are even higher, since individual imprint defects are the root source of extended defects in the coalesced templates and hence significantly decrease the usage of the wafer or even render the wafer useless for LED overgrowth. Therefore, numerous experiments regarding the etch process of the nanorods were performed. Example is given by the chemical component of the dry etch method. Experiments have been undertaken to try to decrease the Cl2/Ar etch rate of a silicone acrylate based resist formulation. Samples were O2 plasma etched at UoB. Water and bromonaphthalene contact angles of the samples were taken as shown in Fig. 5.2 on the left. To see if the change in surface chemistry corresponds in a change in Cl2/Ar etch resistance, the 0 min, 10 min and 30 min O2 etched samples were subjected to 30 s, 60 s and 90 s Cl2/Ar ICP etching at a Cl2 flow rate of 15 sccm, an Ar flow rate of 5 sccm, a forward power of 250 W, a process pressure of 4 m Torr resulting in a DC bias of 260-290 V. The right of figure 5.2 shows these results. It can be seen that the etch rate has not changed so any oxide layer is likely to be very thin.

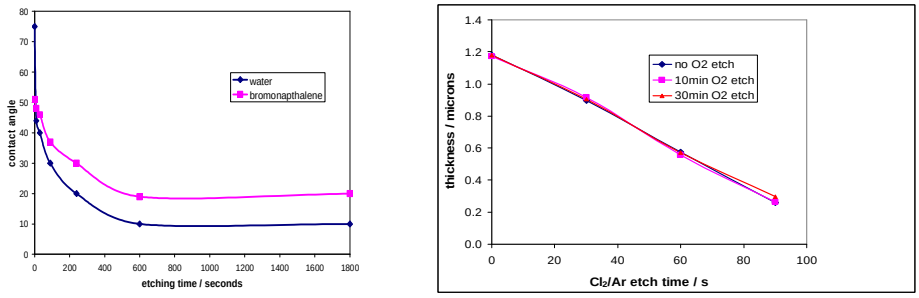

Figure 5.2: Left: Contact angle vs. etch time. Right: Etch time vs. surface chemistry.

Part of the progress in the nanorod formation was backed by developing etch hardware capable of taking the etch processes towards exploitation (OIPT). The new area in this project was GaN etching, where etch tools are still relatively immature. The target for exploitation is also changing, because the wafer size for manufacture is moving from 2” to 4”, 6” and even larger. OIPT has explored two development options:

1) A large area etch tool, capable of processing up to 60 x 2” wafers. This has required the development of a novel plasma source, capable of delivering a uniform ion/radical mixture to a carrier plate of 490mm diameter.

2) A single wafer etch tool capable of taking 100mm substrates (and compatible with future developments supporting sizes up to 200mm). The new aspect here was the etch table: an electrostatic wafer holder (electrostatic chuck (ESC)) for sapphire wafers was not generally available and needed development.

Based on the developed processes, an etch rate on GaN pieces of 1.8µm/min was achieved with a selectivity of 0.9:1 to photoresist. On full 100mm wafers with nanocolumn patterning the rate was reduced to 0.52 µm/min.The reproducibility was better than +/-4% over the last batch of project samples as was measured by SEM (see Fig. 5.3). This demonstrated the ability of the developed hardware to deliver the required process.

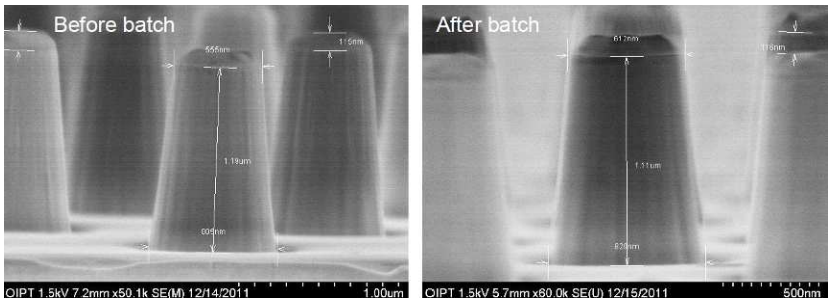

Figure 5.3: SEM images of etched NRs before batch processing (left) and after batch processing (right).

Eventually, the process development enabled the fabrication of High aspect ratio GaN nanostructures (UoB). A new avenue in the work plan is to explore the possibility of creating core-shell structures on etched nanorods. This is because the etched nanorods can be created in a more uniform fashion when compared with grown nanorods and thus are more likely to be able to be fabricated into working devices. TUBS have been exploring the regrowth of quantum well structures onto etched nanorods by MOVPE.

Of course, one of the disadvantages with using etched nanorods is the possible presence of an ion damage layer on the nanorods sidewall which could detrimentally affect the nanorods optical properties. Therefore there has been additional effort at UoB to study the initial growth process to look at the recovery and repair of etch damage before quantum wells are grown. In addition, the introduction of a passivation scheme is considered to reduce parasitic growth, what would reduce the effective height of the core-shell nanorods and even worse, could deteriorate the crystalline quality of the nanostructures. Initial results are positive and are shown in Figure 5.4.

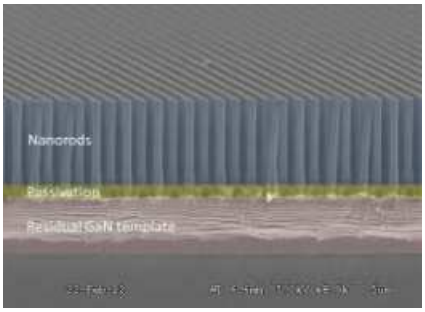

Figure 5.4: Etched nanorods passivated at the base to prevent +c plane growth whilst retaining the conductive residual layer to make a useful device.

Fabrication of LEDs on PNR sapphire templates

The templates were overgrown using a state-of-the-art LED structure at OSRAM OS. The recipe was adjusted in order to compensate for strain in thick epitaxial layers since a problem with peeling off of the epitaxial layer was observed. Furthermore the doping profile of the layer stack was optimized in order to achieve better contact resistance and current spreading.

The limited amount of PNR templates on sapphire delivered from WP3 partners were overgrown with an LED layer structure. The LED wafers were processed using a modified chip process flow based on OSRAM OS's UX:3® thin film technology. One of the characteristics of the UX:3® is that p- and n-contact are realized from the p-side. The n-side is contacted by via-holes etched through the p-side and insulated against it. Several critical issues uniquely to overgrown PNR templates could be identified during chip process:

- sticking of metallization: due to the rough surface stemming most likely from defects introduced during imprint and nanorod fabrication (ranging from large scratches to pits due to missing nanorods) the metallization sticking behavior was inferior leading to problems after wafer bonding (loss due to delamination of bonded epi layer)
- wet chemical treatment: at cracks and epi defects a wet chemical etch, e.g. used for surface roughening to improve light outcoupling, can possibly enter the nanorod layer and hence overetch the structure which leading to device failure
- carbon contamination at nanorod layer: after mesa definition a net-like structure was visible in the mesa trench which mainly consisted of carbon most likely introduced during imprint (cf. Fig 5.5). The carbon net structure was removed in order to prevent short circuits.

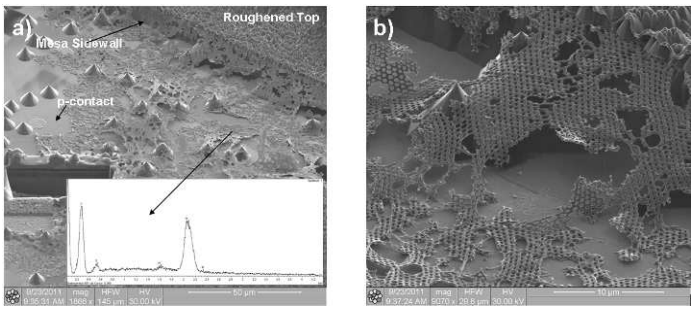

Figure 5.5: a) SEM image of a mesa trench after mesa etching. Pyramids and a net-like structure are visible. The inset shows the EDX measurement of the net-like feature. It consists mainly of carbon. b) Magnification of the mesa sidewall. The net like structure exits the sidewall at the height of the PNR layer.

Several samples were assembled using OSRAM OS's Golden Dragon Plus® package. At standard operation currents of 350 mA the devices showed a total light output of 500 mW with a forward voltage of 3.36 V resulting in a wall-plug efficiency of greater than 42 %. Using OSRAM OS's Ultra White Premium® phosphor those chips can emit up to 122 lumens at standard operating conditions and a correlated color temperature of 5600 K which

corresponds to an efficacy of over 103 lm/W for best samples fulfilling the specifications for milestone M5.1. For color coordinates distant from the Planckian locus, optimized for high system efficacy, best samples can reach efficacies of over 115 lm/W at a corresponding color temperature of 4500 K.

Fabrication of LEDs on PNR silicon templates (OSRAM)

Two fully coalesced PNR templates on silicon have been delivered from WP3 partners and were afterwards succesfully overgrown at OSRAM. Strain management on silicon substrates is far more crucial during the MOVPE growth process due to the difference of the temperature expansion coefficient of GaN and silicon. The tensile strain introduced during cool down after epitaxy can lead to concavely bowed wafers which are therefore prone to cracking. In order to prevent cracking it is necessary to build up enough compressive strain during epitaxial growth of the GaN layers.

Overgrowth of the first PNR template resulted in a high amount of cracks even though several test runs with 2D templates were performed to insure best conditions. Therefore the layer stack and growth parameters were adjusted. An additional AlN interlayer was introduced in order to build up more compressive strain in the coalesced epi-layer. This lead to a vastly improved surface quality as can be seen in Fig. 5.6 which shows the surfaces of the two growth runs.

The surface of the initial PNR templates showed a high amount of circular surface features of about 200nm height as can be seen in Fig. 5.6. In order to get a flat surface for growth of the active layer and subsequent chip processing a 300nm undoped GaN layer was grown. After growth no circular features could be observed.

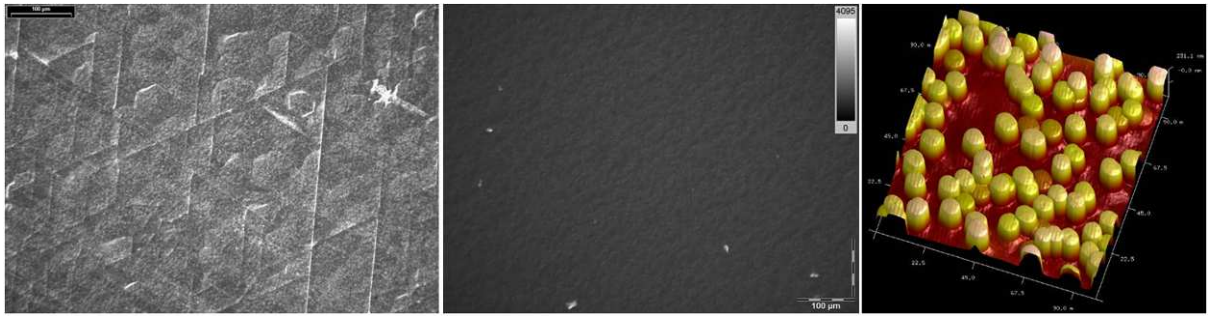

Figure 5.6: Left: Normaski microscopy image of NAV_00928 showing a high amount of cracks. Middle: Normaski microscopy image of NAV_00942 without cracks due to improved strain management. Right: 100µmx100µm AFM scan of the initial surface showing circular features of > 200nm height, which could be overgrown.

The chip process was started but will not be finished by the end of the project deadline. Therefore the deliverable D5.8 and the milestone M5.6 can not be fulfilled in time due to the lack of suitable demonstrators showing 150lm/W on silicon. Optimized growth was shown for 2 and 4inch on sapphire as well for 4inch on silicon.

Fabrication of Nano-LEDs from Nanorod Emitter Arrays

As a test vehicle for chip processing self assembled NRs were processed into LED chips using a thin film like approach. The axial NR LED structures were grown at PDI on 2inch silicon wafers without position control or GaN buffer yielding dense array of nanorods with diameters of ~60 nm. The chip process flow is shown in Fig. 5.7. For passivation and planarization the structures were filled with aluminium oxide using highly conformal atomic layer deposition (ALD). Since the spacing between single NRs is very narrow (<100nm) and less than the height of the NRs a thin layer can be used to fill the array completely. A FIB cut confirmed that the filling covers all NR sidewalls, only few cavities were observed which do not impede the chip process or device functionality. Back etching of the AlOx layer was performed using phosphorous acid in order to expose the p-GaN tips for contacting. A metal stack was deposited as p-contact consisting of ITO as initial contact layer and for further planarization, an Ag-layer acting as mirror and a solder-layer in order to bond the wafer to a new carrier. After bonding the initial growth substrate was removed using a fluorine-based ICP RIE process in order to expose the n-GaN NR base. The n-contact was realized using ITO as transparent current spreading layer and an Au-containing bond pad for wire bonding. Singulation was realized by laser cutting. The chips were mounted onto TO18 sample holders and characterized.

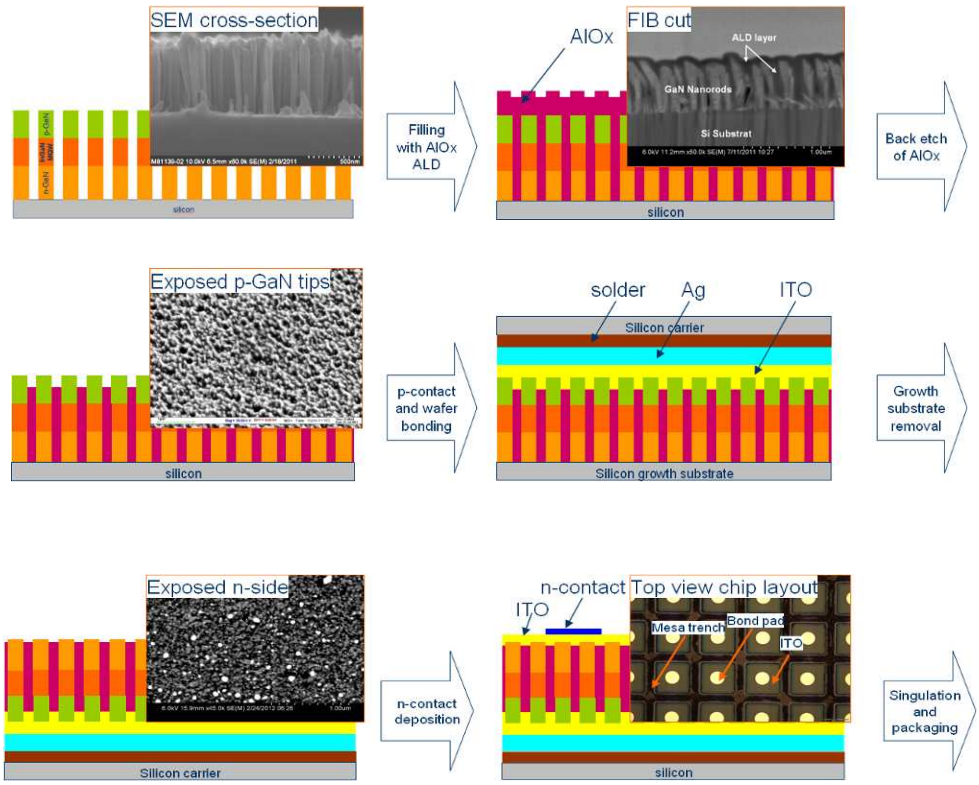

Figure 5.7: Process flow for axial NR LED structures grown directly on silicon without GaN-buffer layer.

Figure 5.8 shows the electroluminescence image of the final chip after packaging. At higher magnifications one can distinguish single NRs emitting in slightly different colors.

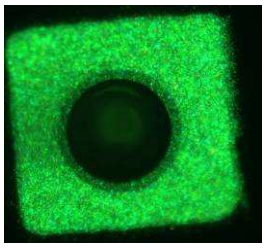

Figure 5.8: Electroluminescence image of a packaged NR LED thin film chip (300µm square chip on TO18 mount).

A comparable chip process was started for several axial NR samples grown by UPM emitting in different colors and phosphor-less white. Those structures were grown on an n-GaN buffer using position control via a thin Ti-mask which was structured by colloidal dot lithography. Since those structures show a variation of different spacing between single NRs, some gaps even exceeding the height of the NRs, a single thin layer deposited by ALD is not suitable for filling. In this case the back etching to expose the tips of the NRs would open holes in the passivation layer which would result in short circuits of p- and n-contact. The deposition of one thick, conformal layer is unsuitable as well since the etching process in order to expose the GaN tips only is difficult to control. Hence, a double layer process was introduced consisting of an initial thin layer of AlOx ALD and a second thick layer of conformal deposited SiO2. The two layers can be etched selectively, allowing a very good control of the etching depth. SEM images of those different steps can be seen in Fig. 5.9.

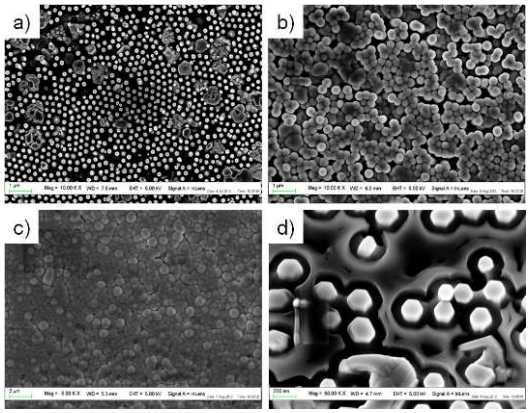

Figure 5.9: SEM images of different filling steps. a) Bare NR wafer showing different NR distances. b) After a thin layer of ALD deposition some gaps persist. c) After deposition of an additional thick, conformal layer all gaps close. d) Selective back etch allows good controllability of p-GaN tip exposure (here: 30°tilt).

The chip process for those samples will be finished after the end of the reporting deadline; hence the milestones M5.3, M5.5 and M5.6 as well as the deliverable D5.8 could not be

fulfilled yet. Considering the quality of the applied NR emitter structures, it is very likely that M5.3, M5.6 and D5.8 will be met with some delay.

For the second type of nanoemitter, the core-shell nanorods, a concept and proof of a feasible chip process was provided. Therefore, it was necessary, to develop schemes for GaN nano-emitter processing (TUBS) including contacting of core-shell LED arrays, filling and substrate removal and Laser lift-off of core-shell LED structures.

One approach to contact core-shell LED structures at TUBS is to separate two metal contacts by cyclotene filled between the LED structures in order to contact the bottom (or lower sidewall) and top of the structures in an array. Such suitable filling of grown core-shell structures is difficult due to the inhomogeneous structure geometry. At shorter structures the top facet is covered (see Fig. 5.10), if a structure is missing or very short the filling height is vanishing at this position and in result a shortcut of the two contact metals can occur.

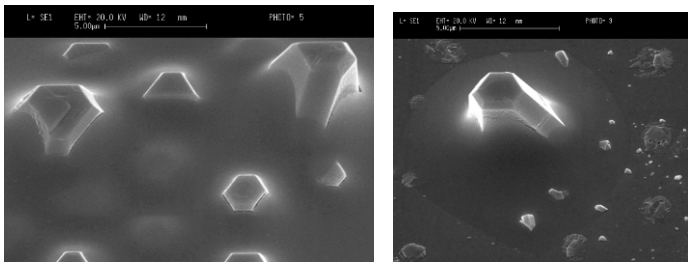

Figure 5.10: SE images of inhomogeneous core-shell LED rods on sapphire (on a pattern with intended diameter of 400nm and distance of 5 µm) after cyclotene filling, ICP etching and Au evaporation, at tilt=30°.

TUBS combined cyclotene filling with a transfer into silver powder (flip chip process) in order to prove if this is an option to perform electrical contacts to an array of core-shell LED rods grown on nonconductive substrate. The cyclotene will insert a constant distance between the top and bottom contact.

An evaporated and annealed metal layer is used to enhance the sticking between the GaN structures and Ag powder. Due to shadow of the structure in evaporation of 30 nm Pd + 300 nm Au (and later a second evaporation of 100nm Au) the metal thickness on the substrate is reduced. This result in steps inside the cyclotene close to the structures which are observed after the transfer by AFM and SEM, the structures are looking out of the cyclotene about 400nm which fits to the metal thickness.

At arrays of core-shell LEDs covered by Au and pressed into silver powder on a silicon wafer, the sapphire substrate was successfully removed by performing laser lift-off at OSRAM. Afterwards, TUBS examined the different patterns using BSE images (sum of a 4QBSE-detector) and crosschecked them by EDX.

In Fig. 5.11, areas colored in green are indicating Gold, violet areas are indicating Gallium (or GaN). The silver powder is not visible in this view, but the former bottom part of the LED rods is strongly damaged, holes through the whole structure are visible at some rods and some gold and gallium balls are placed on them.

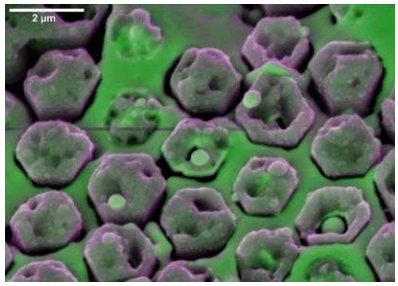

Figure 5.11: SE image (brightness) color-coded by a symmetric BSE image of Au coated GaN LED structures sticking in silver powder after performing laser lift-off at tilt = 30°.